Practical Applications of Cosmic Ray Science: Spacecraft, Aircraft, Ground Based Computation and Control Systems and Human Health and Safety

ICED 2012 Mars Habitat Design Program - Sustaining Humans in Mars.
Blackstone Valley Tech.
December 12, 2012

First presented at CR 2012 Symposium, University of Denver, Denver, Colorado
June 26 - 28, 2012

William Atwell - Boeing Research & Technology, Houston, Texas
Steve Koontz - NASA, Johnson Space Center, Houston, Texas
Eugene Normand - Boeing Research & Technology, Seattle, Washington

1

Outline

- Outline and Abstract
- **1) Cosmic ray interactions with matter**
  - Direct Ionization/Excitation Particle Tracks
  - Nuclear Reactions and Secondary Particle Showers (and more ionization tracks)
- **2) Cosmic Ray Exposure Environments**
  - Earth surface and atmosphere
  - Low Earth Orbit (International Space Station)
  - Interplanetary Space
- **3) Cosmic ray effects on contemporary electronic technology**
  - Ground based computation and control system effects
  - Commercial and military aircraft electronics systems effects
  - Spacecraft electronic systems effects
- **4) Cosmic ray effects on human health and safety**
  - Earth Surface Environments
  - Commercial and Military Aircraft Environments
  - Manned Spaceflight Environments
- **5) Summary and Conclusions**
- **6) Supporting Information and References**

1.0: Cosmic Ray Interactions with Matter

The natural space radiation environment consists primarily of energetic charged particles: Galactic cosmic rays, solar cosmic rays, and magnetically trapped radiation (2,4)

**Energetic charged particle interactions with target materials:
three basic processes**

1. Energy loss (dE/dx) by direct ionization/excitation of material along the particle track
   - Direct ionization effects – linear energy transfer (LET) – "slowing down"
   - Primary cause of single event effects (SEE) in susceptible electronic devices
   - Primary cause of total ionizing dose effects in susceptible electronic devices
   - Primary cause of human health effects

2. High energy collisions (inelastic/hadronic) triggering nuclear reactions
   - Nuclear hadronic reactions initiate secondary particle showers in the target mass
   - Further collisions of secondary particles with target nuclei lead to expansion and propagation of the secondary particle shower
   - Secondary particles can produce direct ionization and more nuclear reactions

3. Collisions with material nuclei that produce displacement damage
   - Displacement of target atoms so as to disrupt crystal structure (solids only – not considered further here, but important for some spacecraft optoelectronics)

1.1: GCR Exposure Environments: Earth Surface and Atmospheric Environments: Dominated by secondary particle showers

Earth surface/atmospheric environments

-1000 grams/cm^2 air shielding mass at sea level
-latitude dependent geomagnetic shielding
-GCR secondary particle shower products dominate

Commercial and military aviation environments

-Altitude dependent air shielding mass
-latitude dependent geomagnetic shielding
-Solar cycle modulation of GCR environment
-Latitude dependent solar particle event exposure
-Pfotzer secondary shower particle maximum at about 20 km altitude (mid latitudes)
-Average ISS hourly crew dose rates are on the order of 20 μSv/hr - comparable to commercial aircraft dose rates on polar routes at solar minimum

Image Credit -The Boeing Company
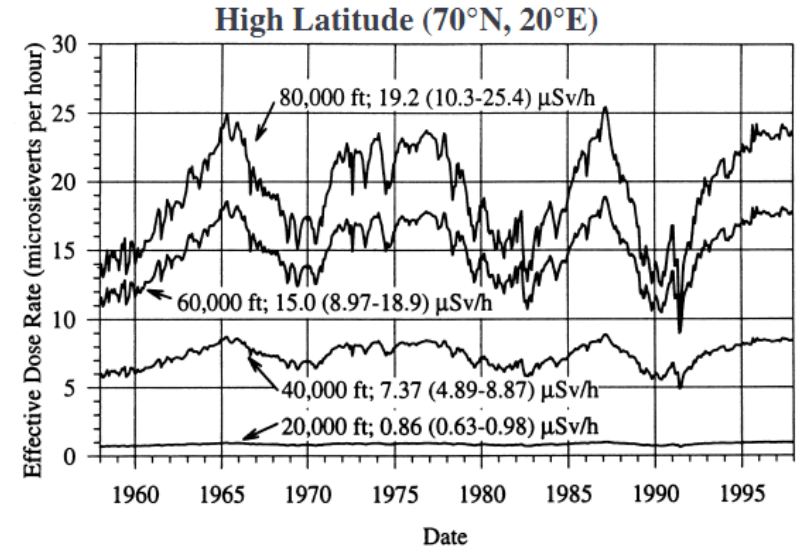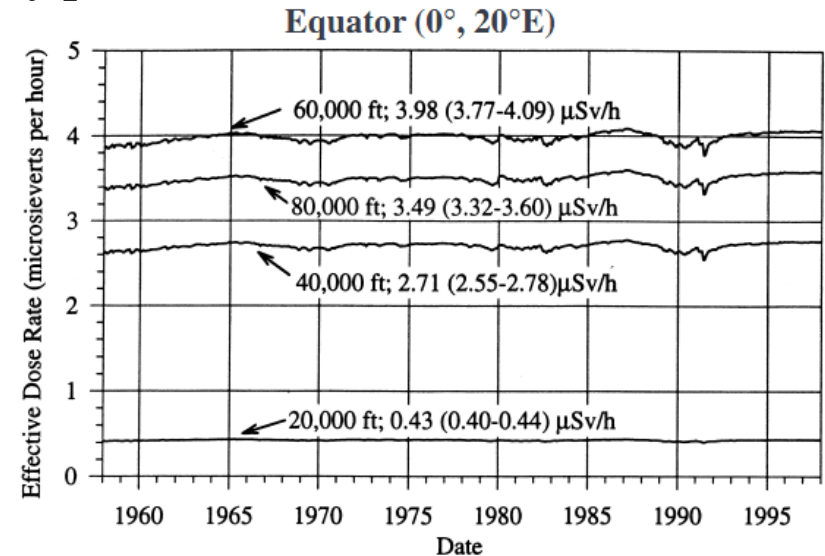
Susan Bailey, "Air Crew Radiation Exposure and Overview," Nuclear News, pp 32-40, January 2000
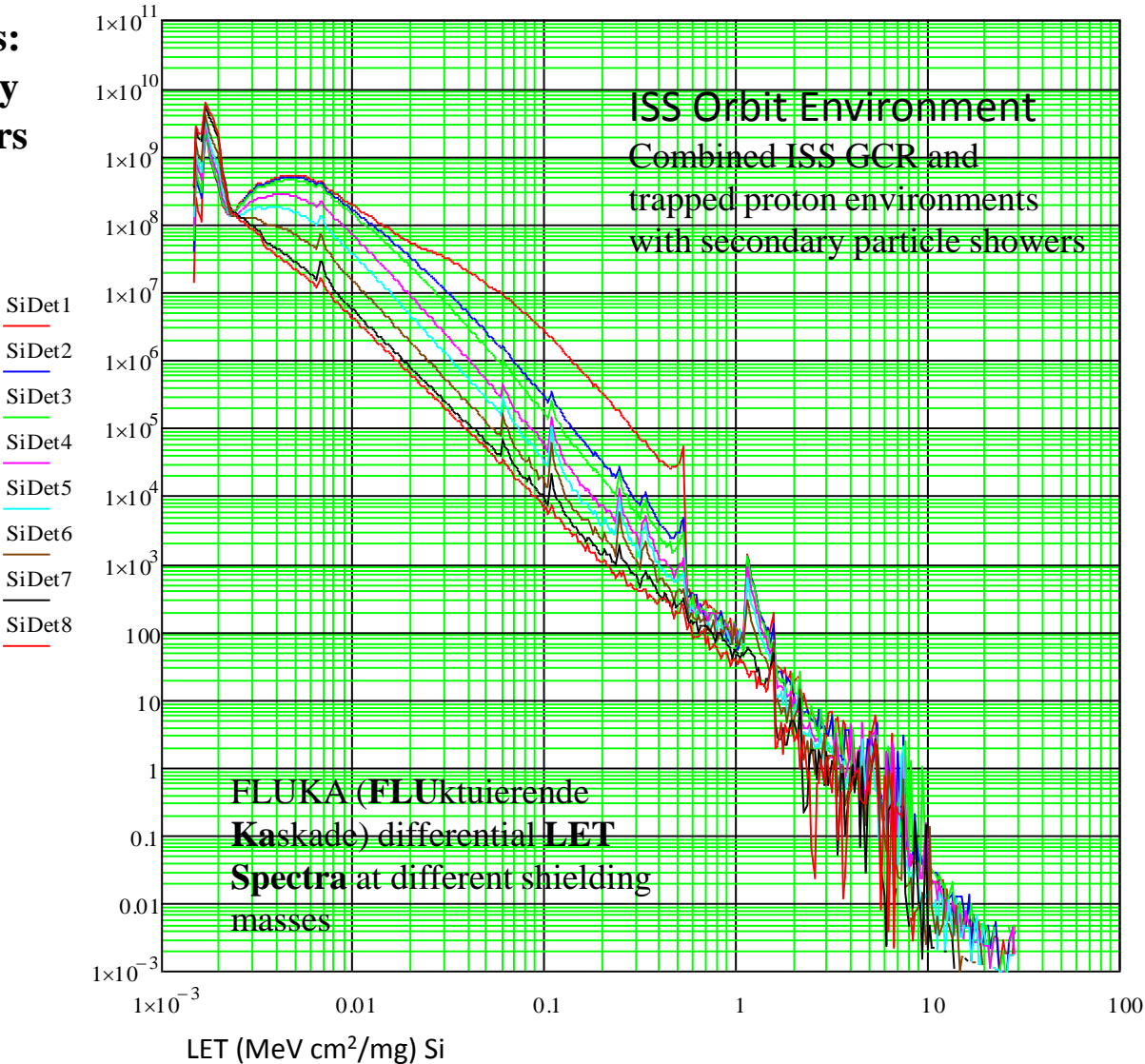http://www.ans.org/pubs/magazines/nn/docs/2000-1-3.pdf

1.2: GCR Exposure Environments: Low Earth Orbit (LEO) – Primary CR and secondary particle showers

The differential LET spectra [#/(cm^2 week LET)] at various shielding depths in a concentric spherical shell model spacecraft is shown to the right.

LET spectra are calculated, using the FLUKA (1) Monte Carlo radiation transport code, as the number of particles entering each of the Si detector shells placed at various depths in the concentric spherical shell model (see the table below).

All secondary particle shower processes are enabled and full shielding mass distribution function for each Si shell is utilized in a fully three dimensional calculation. Total ionizing dose and nuclear reactions "star" density is also calculated but not reported here.

ISS Orbit Environment
Combined ISS GCR and trapped proton environments with secondary particle showers

FLUKA (**FLU**ktuierende **Ka**skade) differential **LET Spectra** at different shielding masses

LET (MeV cm^2/mg) Si

SiDet1
SiDet2
SiDet3
SiDet4
SiDet5
SiDet6
SiDet7
SiDet8

Steve Koontz, Brandon Reddell, Paul Boeder: "Calculating Spacecraft single Event Environments with FLUKA, Paper W-33, Proceedings of the 2011 NSREC Radiation Effects Data Workshop, IEEE, July 2011
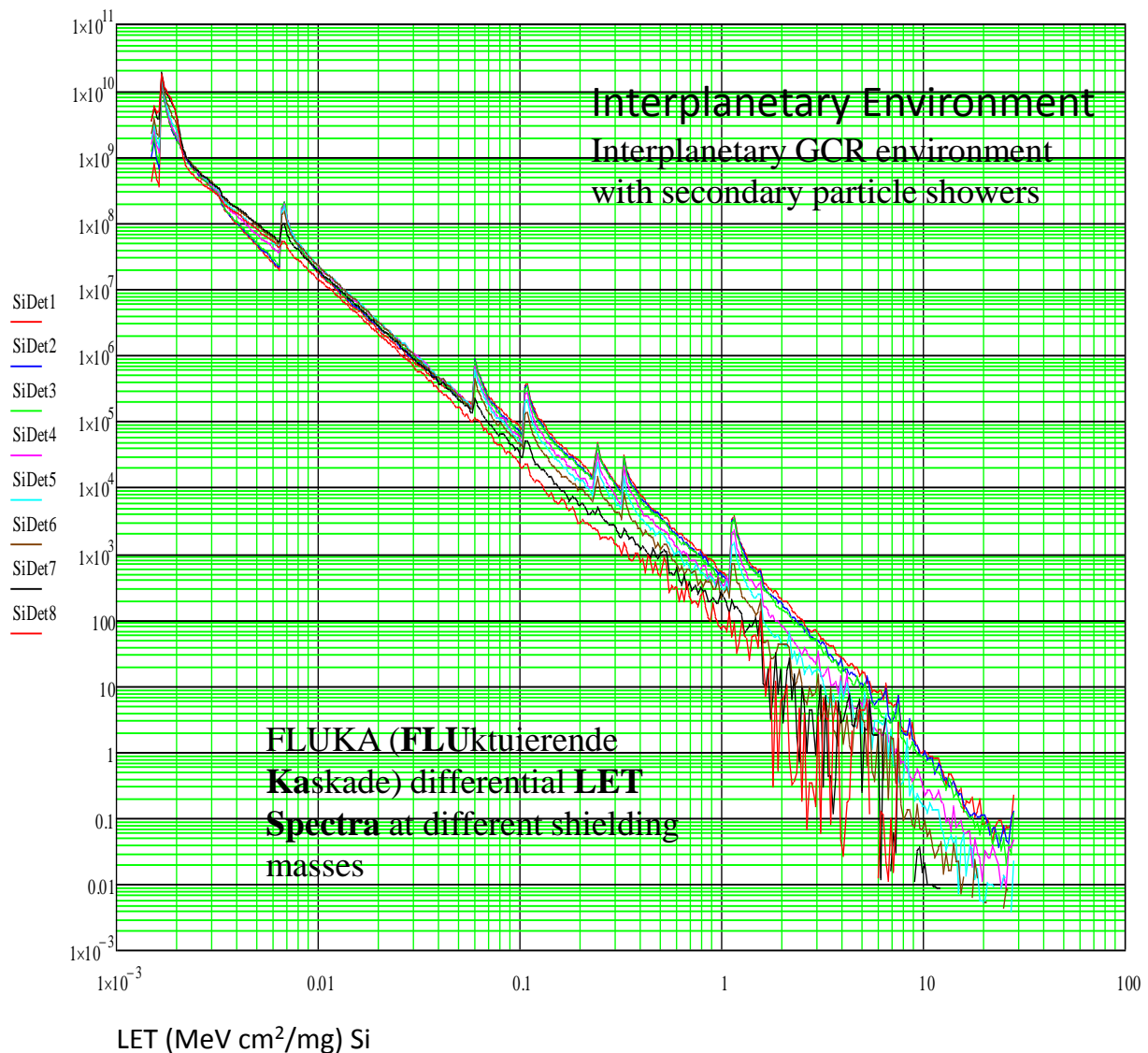
Detector Si Shell	SiDet1	SiDet2	SiDet3	SiDet4	SiDet5	SiDet6	SiDet7	SiDet8
Detector Shell Radius (cm)	5037.4	5037.3	5037.1	5035.6	5033.7	5030.0	5018.9	5000.0
Si Detector Median Al Shielding Mass in g/cm^2	0.15	0.81	1.6	7.9	15.6	31.1	77.5	156.2

1.3 GCR Exposure Environments: Interplanetary Environment – Primary CR and secondary particle showers

The differential LET spectra [#/(cm² week LET)] at various shielding depths in a concentric spherical shell model spacecraft is shown to the right.

LET spectra are calculated, using the FLUKA (1) Monte Carlo radiation transport code, as the number of particles entering each of the Si detector shells placed at various depths in the concentric spherical shell model (see the table below).

All secondary particle shower processes are enabled and the full shielding mass distribution function for each Si shell is utilized in a fully three dimensional calculation. Total ionizing dose and nuclear reactions "star" density is also calculated but not reported here.

Steve Koontz, Brandon Reddell, Paul Boeder: "Calculating Spacecraft single Event Environments with FLUKA, Paper W-33, Proceedings of the 2011 NSREC Radiation Effects Data Workshop, IEEE, July 2011

Interplanetary Environment
Interplanetary GCR environment with secondary particle showers

FLUKA (**FLU**ktuierende **Ka**skade) differential **LET Spectra** at different shielding masses

LET (MeV cm²/mg) Si

Legend: SiDet1, SiDet2, SiDet3, SiDet4, SiDet5, SiDet6, SiDet7, SiDet8

Detector Si Shell	SiDet1	SiDet2	SiDet3	SiDet4	SiDet5	SiDet6	SiDet7	SiDet8
Detector Shell Radius (cm)	5037.4	5037.3	5037.1	5035.6	5033.7	5030.0	5018.9	5000.0
Si Detector Median Al Shielding Mass in g/cm²	0.15	0.81	1.6	7.9	15.6	31.1	77.5	156.2

Solid state electronic devices as charged particle detectors: Single Event Effects (SEE)

Schematics of a solid state charged particle detector (right) and a MOSFET transistor (left) illustrating the particle counting or single event upset process. Direct ionization by CR charged particles and charged particles produced by nuclear reactions in the device can produce counts in the detector and SEE events in the transistor only if the devices are powered, i.e. only if an electric field is applied to force charge collection.

http://nsspi.tamu.edu/nsep/courses/basic-radiation-detection/semiconductor-detectors
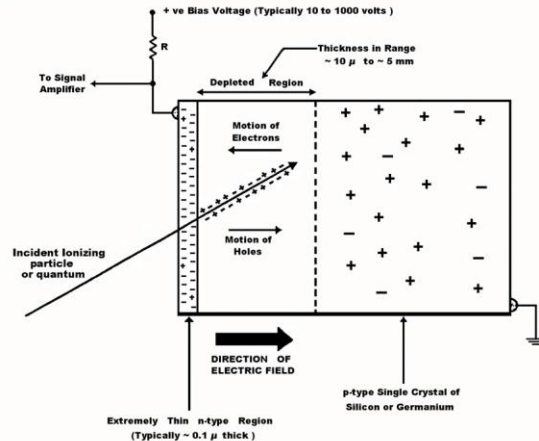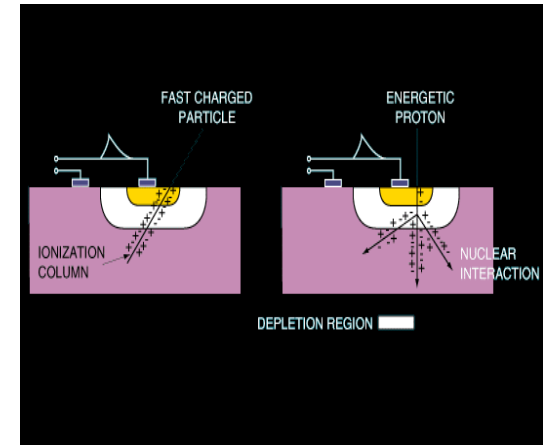

Lauriente, M., Vampola, Al. L., "Spacecraft anomalies due to radiation environment in space," NASDA/JAERI 2nd International Workshop on Radiation Effects of Semiconductor Devices for Space Applications, Tokyo, Japan, March 1996.

Solid state electronic devices as charged particle detectors: Total Ionizing Dose (TID) Effects

Schematic of n-channel MOSFET illustrating radiation-induced charging of the gate oxide: (a) normal operation and (b) post-irradiation. The electrostatic field produced by trapped charge in SiOx layers changes device characteristics. TID damge accumulated even if the device is unpowered.
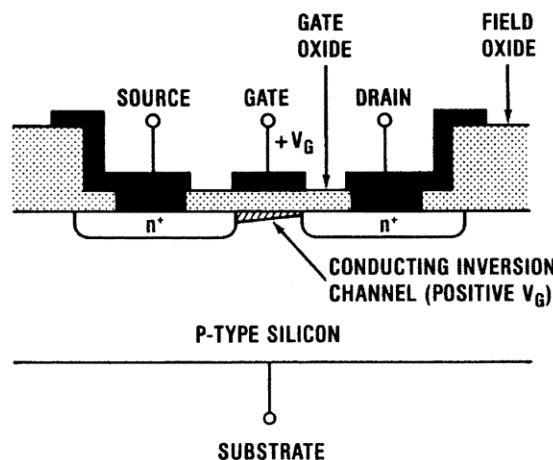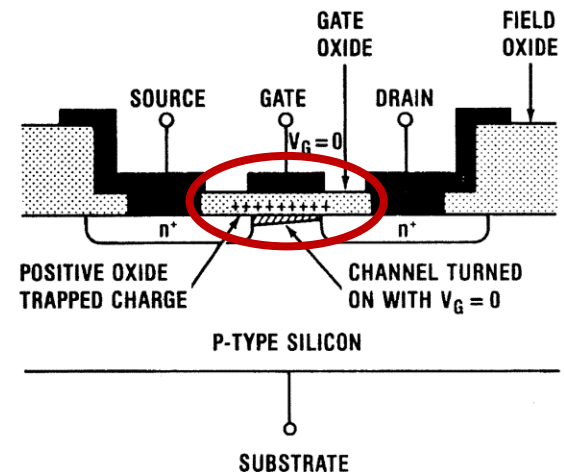
T. R. Oldham, F. B. McLean; "Total Ionizing Dose Effects in MOS Oxides and Devices," IEEE Transactions on Nuclear Science, Vol. 50, No. 3, pp 483-499, June 2003

- **Ground based computation and control systems**
  - SEE caused principally by GCR shower generated secondary neutrons
  - TID effects negligible in the natural environment

- **Aircraft electronic systems**
  - SEE caused principally by GCR shower generated secondary neutrons and protons
  - TID Effects negligible in the natural environment

- **Spacecraft electronic systems**
  - Single event effects caused principally by GCR heavy ions, GCR protons, trapped protons, and solar particle events (SPE)
    - Neutrons and other secondary shower particles increasingly important as spacecraft shielding mass increases, especially when the electronic device contains heavy elements - e.g. Pb, Hf, W
  - TID effects are important is specific high-dose-rate natural environments, e.g. planetary radiation belts and/or solar particle events

2.1: Ground based computational and control systems - History

- **Observations of satellite electronic anomalies lead to the first report of SEE effects in solid state electronics**
  - D. Binder, E. C. Smith, A. B. Holman; "Satellite anomalies from galactic cosmic rays," IEEE Transactions on Nuclear Science, Vol. NS-22, No. 6., pp 2675-2680, December 1975

- **Memory parity errors observed in the first Cray supercomputer at Los Alamos in 1976 were later determined to be SEUs caused by atmospheric neutrons**
  - E. Normand, J. L. Wert, H. Quin, T. D. Fairbanks, S. Michalak, G. Grinder, P. Iwanchuk, J. Morrison, S. Wender, S. Johnson; "First record of single event upset on ground, Cray-1 Computer at Los Alamos in 1976," IEEE Transactions on Nuclear Science, Vol. 57, No. 6, December 2010

- **Alpha particles emitted from thorium impurities in chip packaging materials were identified as an SEU cause by May and Woods in 1978**
  - T. C. May, M. H. Woods; "A new mechanism for soft errors in dynamic memories," in Proc. Int. Rel. Phys. Symp., April, 1978, pp 33-40

- **Modeling and prediction of cosmic ray effects on computer memories**
  - J. F. Ziegler, W. A. Lanford; "The Effects of Cosmic Rays on Computer Memories," Science, 206, 776, 1979

- **Summary of IBM investigations into soft errors in microelectronic devices**
  - IBM Journal of Research and Development, Vol. 40, Number 1, January 1996

- **JEDEC Standard developed for test and measurement of alpha particle and atmospheric cosmic ray shower induced soft errors in semiconductor devices**
  - Measurement and Reporting of Alpha Particle and Terrestrial Cosmic Ray Induced Soft Errors in Semiconductor Devices, JEDEC Standard JESD89A, October 2006

2.2: Atmospheric Neutron Effects on Ground Based and Aircraft Electronic System Reliability

Ever increasing microelectronic system size, complexity, and capability can lead to overall decrease in Mean Time Between Failure (MTBF) (increase in failures in time (FIT). In 2002, Actel predicted a significant decline in FPGA MTBF with both operational altitude and the scale of the technology node (see below) for Actel field programmable gate arrays (FPGAs)

PROJECTED FAILURE RATE ON SRAM-BASED FPGAS APPLICATIONS DUE TO NEUTRON EFFECTS (ACTEL)

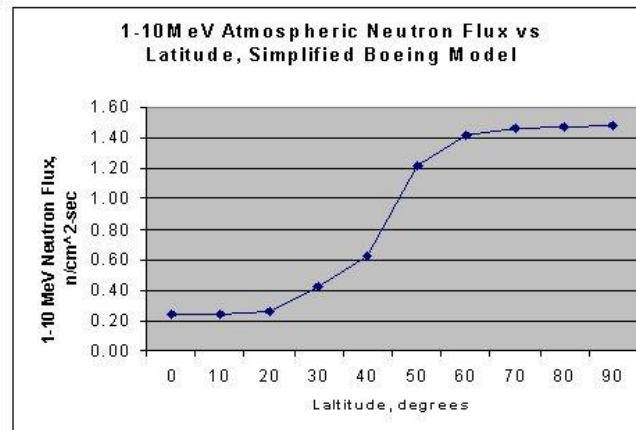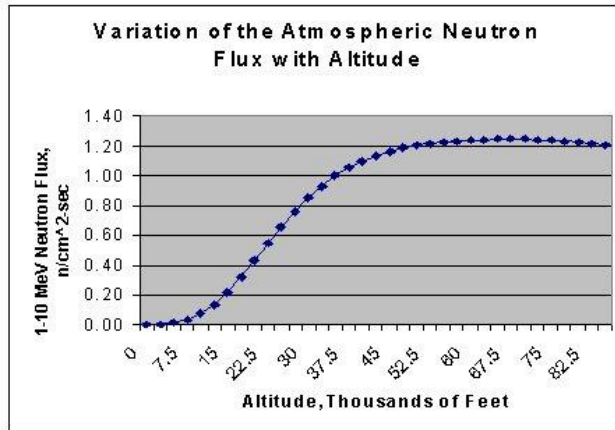| Application Examples	Altitude (feet)	Neutron Flux (relative)	FPGAs/ System	#upsets/1M-gate FPGA/day(.13μ)	MTBF[1] (hours)		FIT[1] (in million)	
					0.13μ	0.09μ	0.13μ	0.09μ
(1) Ground-based Communication Network	5000	1	512	4.19E-4	112	58	8.92	17.24
(2) Civilian Avionics System	30,000	~40	4	1.85E-2	324	162	3.09	6.17
(3) Military Avionics System	60,000	>160	16	8.33E-2	18	9	55.56	111.11

Fan Wang and Vishwani D. Agrawal, "Single Event Upset: An Embedded Tutorial," Proceedings of the 21st International Conference on VLSI Design, IEEE, 2008, DOI 10.1109/VLSI.2008.28

In contrast, XILINX FPGA field performance measurements (the Rosetta Experiment, 2009 - 2012), show soft error rates (MTBF/Mb in 10^6 hrs) decreasing with technology node size for both Configuration and Block RAM, however the advantages of a smaller node can be easily offset by much larger increases in the number of bits in device memory.

Technology node	Product Family	MTBF (10^6 hrs)/Mb Config. Memory	MTBF (10^6 hrs)/Mb Block Memory
90 nm	Spartan-3	5.26	3.4
45nm	Spartan-6	5.41	2.6
28 nm	7 series FPGAs	14.1	17
90 nm	Virtex-4	3.8	2.1
65 nm	Virtex-5	6.1	1.4
40 nm	Virtex-6	9.6	4.0

Data from Xilinx Reliability Report UG116 (v9.0) May 8, 2012, and WP286; www.xilinx.com

2.3: Aircraft Electronic Systems

Variation of the Atmospheric Neutron Flux with Altitude

1-10MeV Atmospheric Neutron Flux vs Latitude, Simplified Boeing Model

Normand, E., Baker, T. J. (1993) "Altitude and Latitude Variations in Avionics SEU and Atmospheric Neutron Flux," *IEEE Transactions on Nuclear Science, vol. 40, No. 6, pp 1484 – 1490, December1993*

| Aircraft	Flight Path	Altitude, ft (×E3)	System	Operat'g Condt'ns	SRAM	# Upset	Meas'd Up/bit-hr	Calct'd Up/bit-hr
E-3	Seattle	29	IBM Exp't	2.5 V	IMS 64K	10	5E-9	4.4-8 E-9
ER-2	N. Cal.	65	IBM Exp't	2.5 V	IMS 64K	12	1.1E-8	1-2 E-8
ER-2	Norway.	65	IBM Exp't	2.5 V	EDI 256K	6	4.6E-9	8-14 E-9
E-3	Europe-1	29	CC-2E	5 V	IMS 64K	53	2.3 E-9	1.8-4.7E-9
E-3	Europe-2	29	CC-2E	5 V	IMS 64K	83	1.6E-9	1.3-2.7E-9
Com'cll Jetliner	Trans-Altlantic	~35	PERF. computer	5 V -	EDI 256K	14	4.8E-8	2.3E-8
F-4	S. Calif.	<25	AP-102	5 V	IMS 64K	4	5.4E-8	3.4E-10
Com'cl Jetliner	World-wide	~33	Avionics computer	5 V	IDT 256K	-----	3.3E-10	5E-10

SEU effects on aircraft avionics systems present a hazard to military and civil aircraft operations, especially in the case of contemporary and future "fly-by-wire" systems, leading to the development of technical standards for management and control of SEE effects in aircraft avionics systems: R. Edwards, C. Dyer, E. Normand; "Technical Standard for Atmospheric Radiation Single Event Effects on Avionics Electronics," Proceedings of NSREC 2004, Radiation Effects Data Workshop, IEEE DOI 10.1109/REDW.2004.1352895 pp 1-5, July 2004

2.4: Spacecraft Electronic Systems

- **The reliability and safety of spacecraft electronic systems are often determined, in practice, by the mission space radiation environment**
  - SEE rate depends on the primary particle flux and the extent of secondary particle production in spacecraft shielding mass
  - TID effects lead to slow degradation of device performance characteristics as dose accumulates during a mission, leading, ultimately, to wear-out like device failure
- **Mitigating SEE/TID effects in spacecraft electronic systems**
  - Selection of electronic parts resistant to SEE/TID
    - Military Class S parts or equivalent
    - Silicon-on-insulator (SOI) device structure for reduced SEU and latch-up sensitivity
    - Not always possible – susceptible complex parts may be the only option for the required performance
  - Design of robust system architectures
    - Triple (or more) module redundancy
    - Error detection and correction firmware and software
    - Fault detection isolation and recovery (FDIR) software systems
- **A rigorous component and integrated system test and analysis program is essential to demonstrate the reliability of the spacecraft electronic system before flight.**
  - Accurate definition of worst-case natural cosmic ray, solar energetic particle event, and trapped radiation flight environments
  - Applicable component and system ground based accelerated test methods
  - Understanding the relationship between ground based test results and expected on-orbit electronic system failure rates
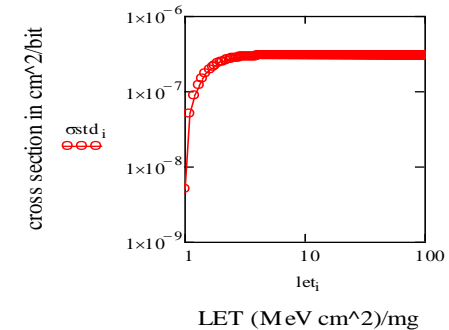
2.5: Estimating SEE rates: Verifying Spacecraft System Safety and Reliability
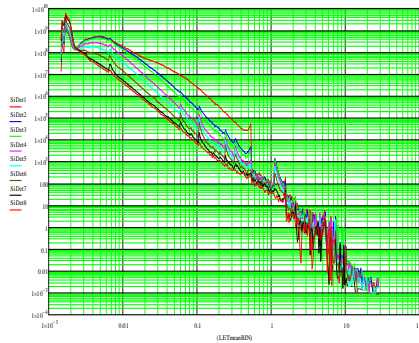
Direct Ionization

References (2 – 10)

LET (MeV cm^2)/mg

Differential LET distribution function (spectrum) calculated for the shielding mass distribution function applicable to the electronic device location in the spacecraft

Electronic device heavy ion accelerator test data - Measured device cross section ($\sigma(LET, \Theta, \Phi)$) vs. Heavy ion effective LET value expressed as an integral Weibull or the integral (cumulative) log normal distribution function, or the tabulated test results data
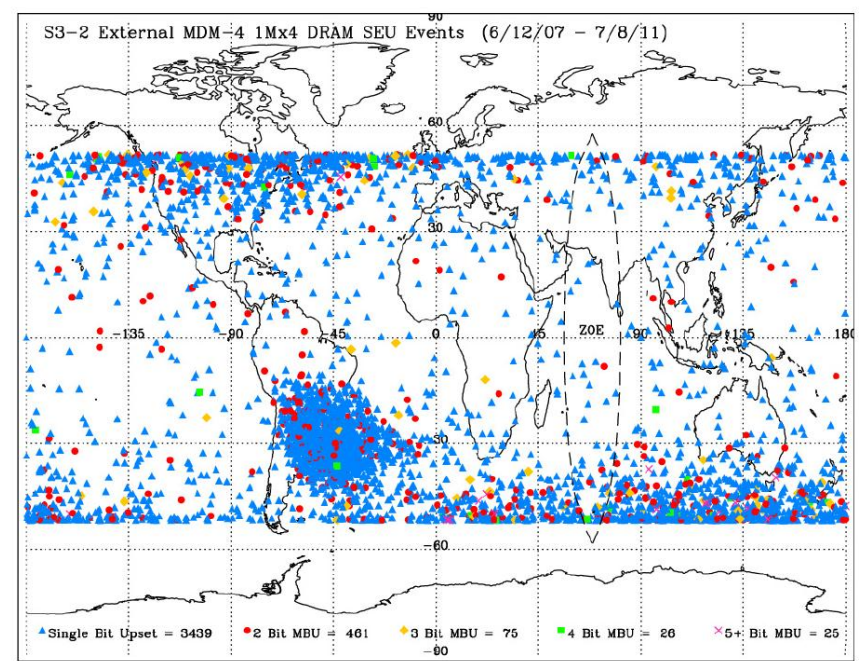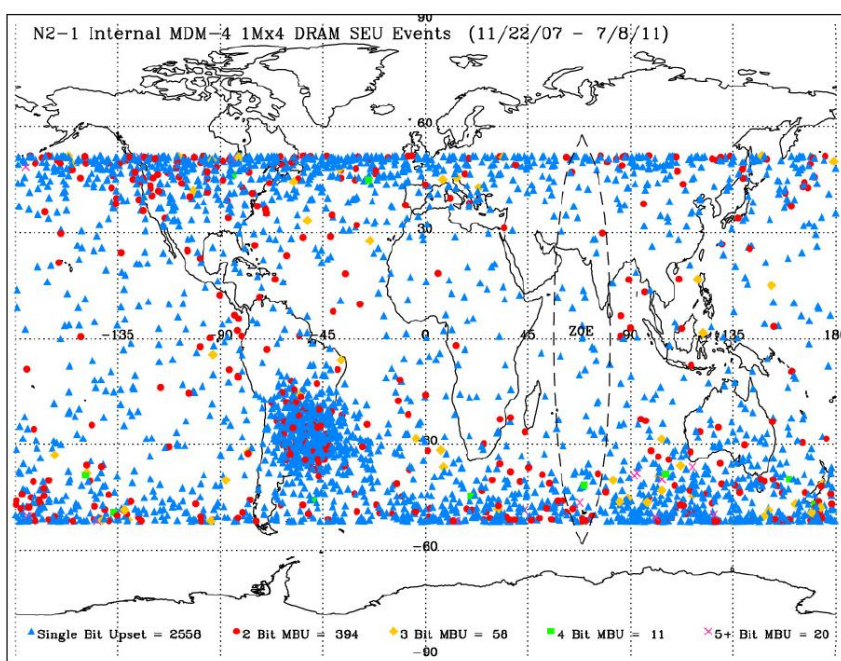
$$\text{SEU Rate} = \iiint f(LET) \times \sigma(LET, \Theta, \Phi)\, d(LET)\, d(\Theta)\, d(\Phi)$$

In-Device Nuclear Reactions
References (2 – 10)

Nuclear reactions internal to the microelectronic device can be triggered by primary and secondary particle (especially those producing little or no direct ionization e.g. neutrons, protons, and pions) inelastic collisions with microelectronic device nuclei to produce high-LET, short-range fragments.

$$\text{SEU Rate} = \sigma(\text{device-particle}) \times \text{Flux (particles/time)} \times \text{number of devices}$$

N2-1 Internal MDM-4 1Mx4 DRAM SEU Events (11/22/07 - 7/8/11)

Single Bit Upset = 2558 2 Bit MBU = 394 3 Bit MBU = 58 4 Bit MBU = 11 5+ Bit MBU = 20

S3-2 External MDM-4 1Mx4 DRAM SEU Events (6/12/07 - 7/8/11)

Single Bit Upset = 3439 2 Bit MBU = 461 3 Bit MBU = 75 4 Bit MBU = 26 5+ Bit MBU = 25

Image/data Credit: NASA

Image/data Credit: NASA

GCR and trapped proton single event upsets detected and corrected by Error Detection And Correction (EDAC) firmware in ISS computer system Dynamic Random Access Memory (DRAM). EDAC operation is part of the nominal system design, not an anomaly.

Image Credit: NASA

2.6: In-flight vs. calculated spacecraft device SEU rates

Steve Koontz, Brandon Reddell, Paul Boeder: "Calculating Spacecraft single Event Environments with FLUKA, Paper W-33, Proceedings of the 2011 NSREC Radiation Effects Data Workshop, IEEE, July 2011
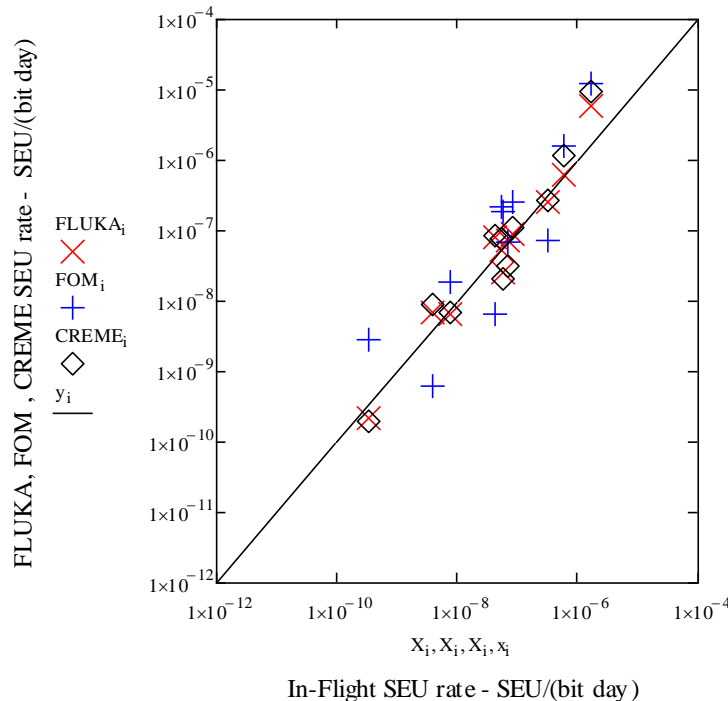
Shielding Mass Rate Ratio =(10 g/cm² Rate)/ (40 g/cm² Rate)

Device	Rate Ratio - Flight	Rate Ratio - FLUKA	Rate Ratio - CREME 96	Rate Ratio - FOM
TI (1M x 4) TMS44400	1.2	1.2	3.5	3.7
TI (4M x 4) TI SMJ41640	0.9	1.8	3.4	5.3

Note that only FLUKA correctly quantifies the shielding mass (i.e. secondary particle shower) effects for the ISS TI CMOS DRAM.

$$\sum_{i}\left[\frac{\left(X_i - FLUKA_i\right)^2}{\left(X_i\right)^2}\right]^{0.5} = 5.7 \qquad \sum_{i}\left[\frac{\left(X_i - CREME_i\right)^2}{\left(X_i\right)^2}\right]^{0.5} = 10.6 \qquad \sum_{i}\left[\frac{\left(X_i - FOM_i\right)^2}{\left(X_i\right)^2}\right]^{0.5} = 26.8$$

Using the same device parameter, the FLUKA based rate calculations show the smallest least squares error and overall acceptable performance compared to CREME-96 and the Peterson FOM, providing some validation for the FLUKA based methods described here.

2.7: FLUKA calculation of the increase in high LET particles entering a thin (10 micron) Si layer from a thin (1 micron) high Z element (W) over-layer as a function of spacecraft aluminum shielding masses (Mercury Messenger SRAM, interplanetary environment)

<u>Y axis</u> - Mercury Messenger SRAM upsets per bit day

$MMRCCrate_i$
×××
$MMRCCrateW_i$
+++

1 µTungsten over-layer

No Tungsten over-layer

$AlmedianCOSvf_i$

For Mercury Messenger SRAM, an SEU rate calculation, based on FLUKA LET spectra calculated for the concentric spherical shell spacecraft model (see back-up), predicts that including a 1 micron Tungsten over-layer above the 10µ Si detector shell should result in a dramatic increase in SEU caused by high LET particles affecting this high threshold device
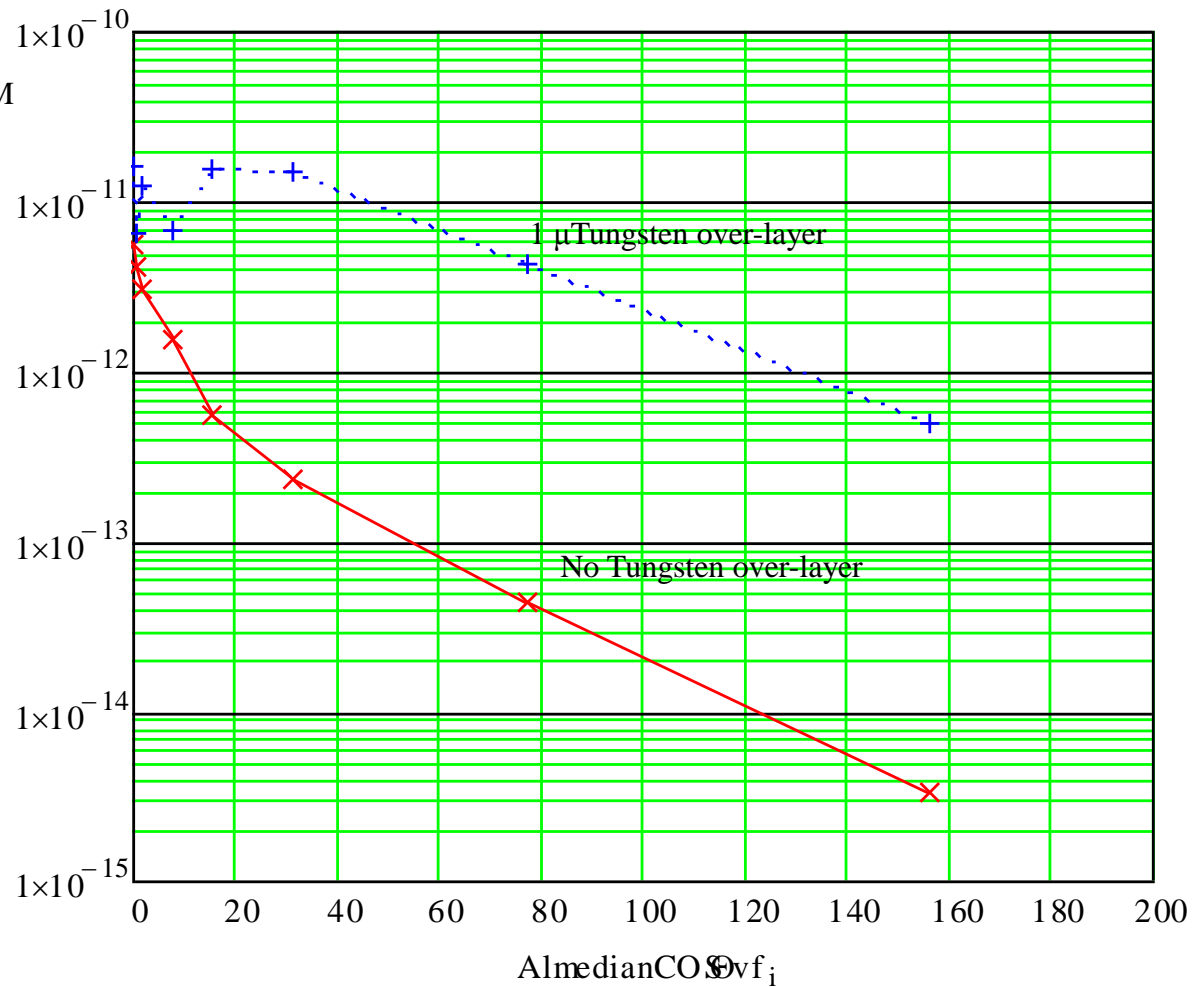
<u>X axis</u> – g/cm^2 Al median shielding mass
(concentric spherical shell target with cosine and solid angle corrections)

2.8: FLUKA calculation of the increase in high LET particles entering a thin (10 micron) Si layer from a thin (1 micron) high Z element over-layer at two different spacecraft aluminum shielding masses
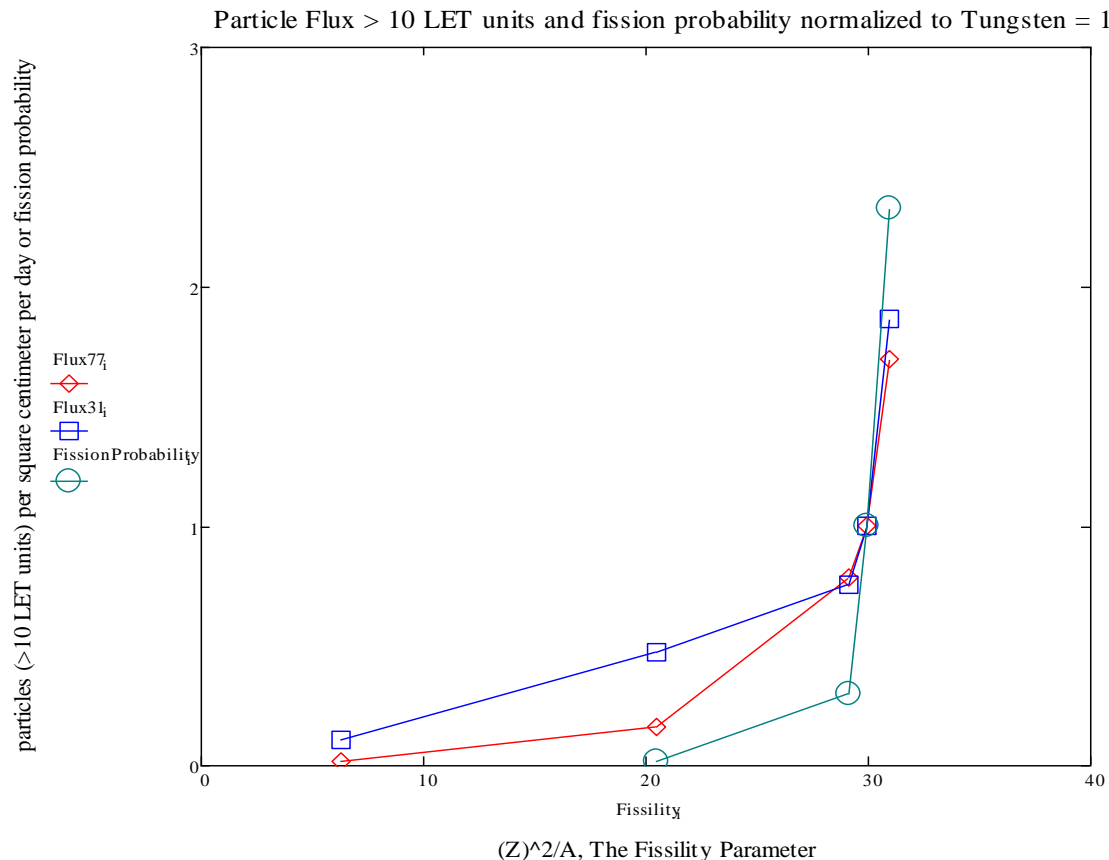
Element	Ag	Hf	W	Pb
Z^2/A	20.434	29.124	29.923	30.918
Relative Fission Probability	0.02	0.3	1	2.3

Particle Flux > 10 LET units and fission probability normalized to Tungsten = 1

particles (>10 LET units) per square centimeter per day or fission probability

Flux77$_i$

Flux31$_i$

FissionProbability

Fissility$_i$

(Z)^2/A, The Fissility Parameter

Explanation

The number of high LET (> 10 MeV cm^2/mg (Si)) particles entering the 10μ Si shells at **median shielding masses of 31 and 77 g/cm^2 Al** correlates with the atomic number of the 1μ high Z element over layer on the Si shell through the fissility parameter, Z^2/A.

Increasing high Z element content in modern semiconductor device structures can lead to unexpectedly high upset or latch-up rates at high spacecraft shielding mass. Fission of high Z element nuclei by secondary particle shower species is the probable cause.

Steve Koontz, Brandon Reddell, Paul Boeder: "Calculating Spacecraft single Event Environments with FLUKA, Paper W-33, Proceedings of the 2011 NSREC Radiation Effects Data Workshop, IEEE, July 2011
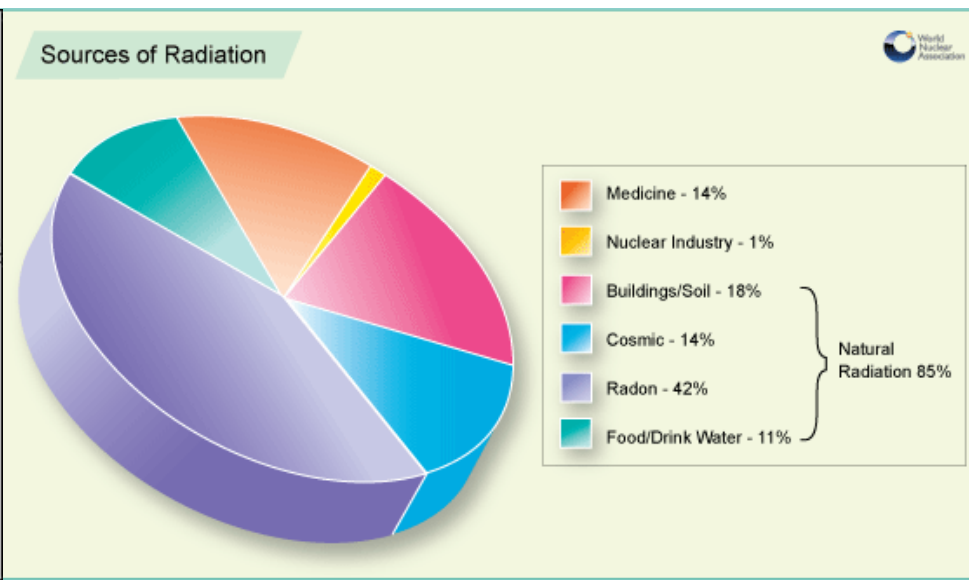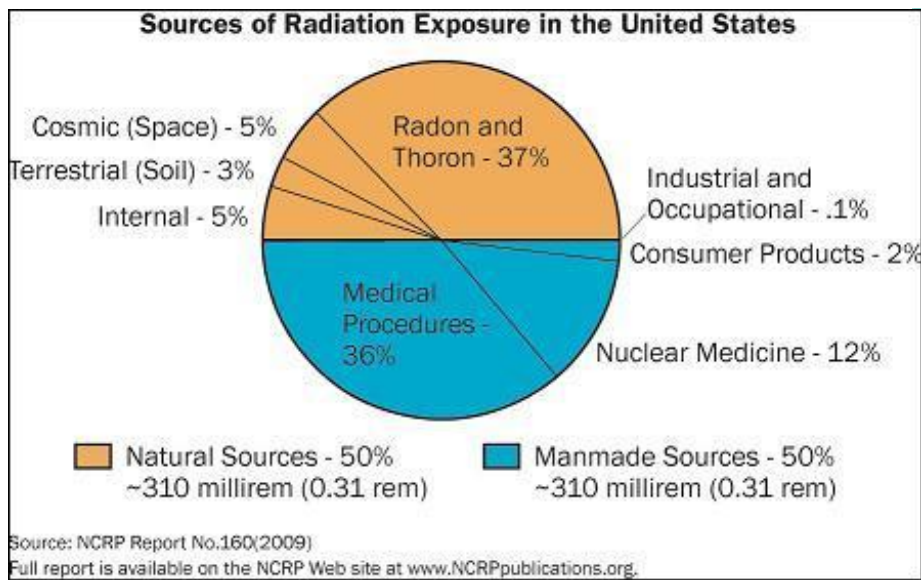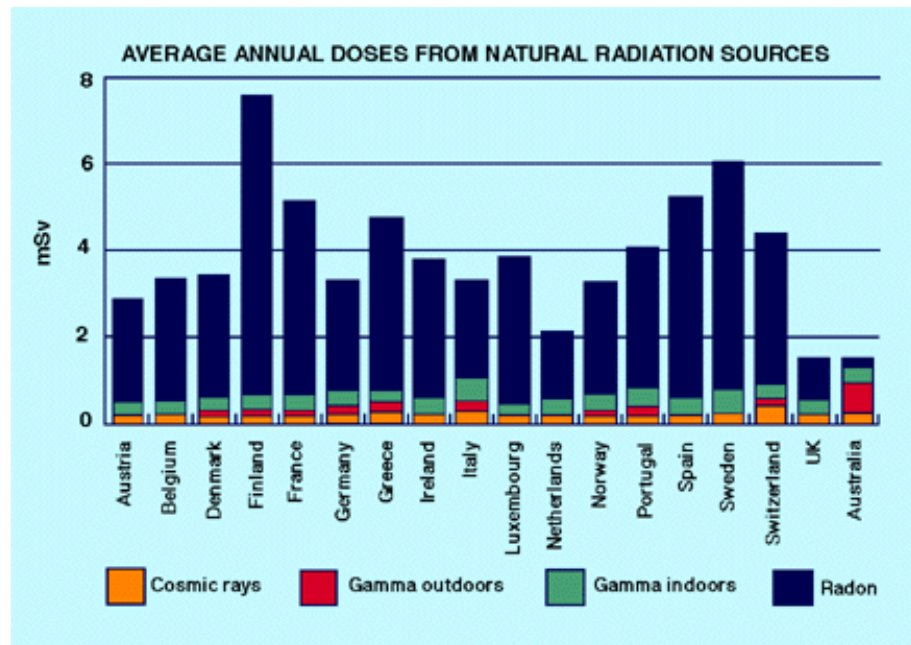
3.0: CR effects on human health and safety

Some comparative (Earth environment) radiation doses and their effects

2.4 mSv/yr	Typical background radiation experienced by everyone (average 1.5 mSv in Australia, 3 mSv in North America).
Up to 5 mSv/yr	**Typical incremental dose for aircrew in middle latitudes.**
9 mSv/yr	**Exposure by airline crew flying the New York – Tokyo polar route.**
20 mSv/yr	Current limit (averaged) for nuclear industry employees and uranium miners.
50 mSv/yr	Former routine limit for nuclear industry employees. It is also the dose rate which arises from natural background levels in several places in Iran, India and Europe.
50 mSv	Allowable short-term dose for emergency workers (IAEA).
100 mSv	Lowest level at which increase in cancer risk is evident (UNSCEAR). Above this, the probability of cancer occurrence (rather than the severity) is assumed to increase with dose.
250 mSv/yr	**Natural background level at Ramsar in Iran, with no identified health effects.**
350 mSv/lifetime	Criterion for relocating people after Chernobyl accident.
500 mSv	Allowable short-term dose for emergency workers taking life-saving actions (IAEA).
1,000 mSv short-term	**Assumed to be likely to cause a fatal cancer many years later in about 5 of every 100 persons exposed to it. If the normal incidence of fatal cancer were 25%, this dose would increase it to 30%.**
1,000 mSv short-term	**Causes (temporary) radiation sickness (Acute Radiation Syndrome) such as nausea and decreased white blood cell count, but not death. Above this, severity of illness increases with dose.**
5,000 mSv short-term	Would kill about half those receiving it within a month.
10,000 mSv short-term	Fatal within a few weeks.

3.1: Biological Effects of Cosmic Radiation – Earth Surface Environments

- Earth surface ionizing radiation dose environments are dominated by natural radioisotope decay and man-made radiation source
  - Radon gas is the most important contributor
- CR contributions are on the order of 10% of the natural environment

AVERAGE ANNUAL DOSES FROM NATURAL RADIATION SOURCES

Sources of Radiation Exposure in the United States

Sources of Radiation

http://www.world-nuclear.org/info/inf05.html

19

3.2a: Biological Effects of Cosmic Radiation – Commercial and Military Aviation Environments – CRs determine the dose rate at high latitude/altitude

http://sol.spacenvironment.net/~nairas/Dose_Rates.html
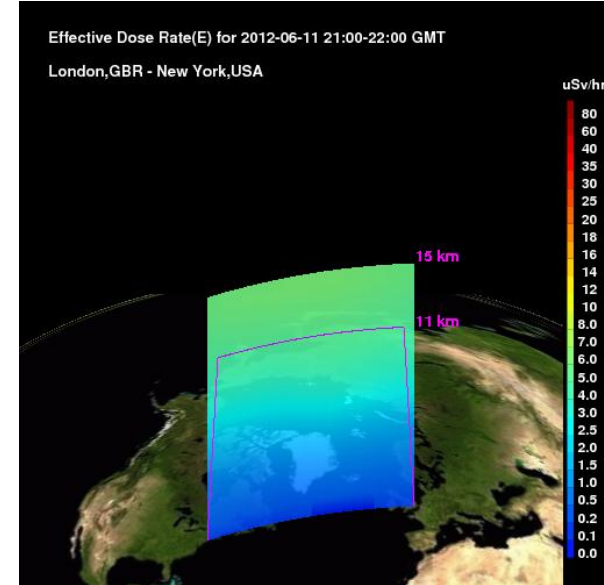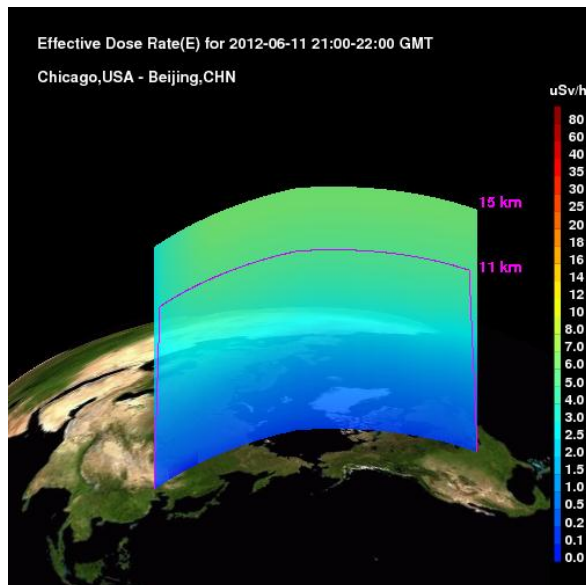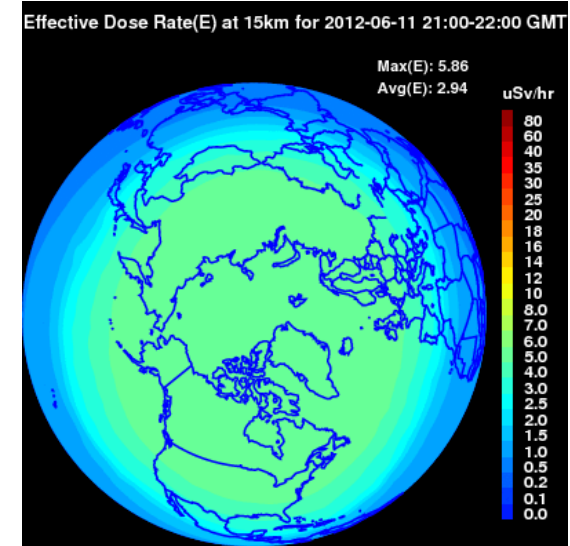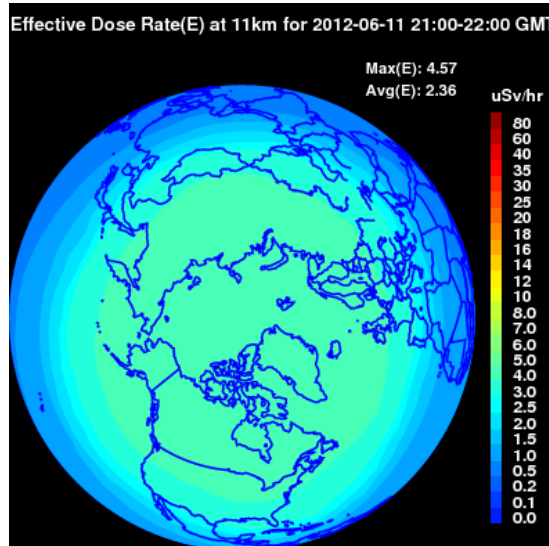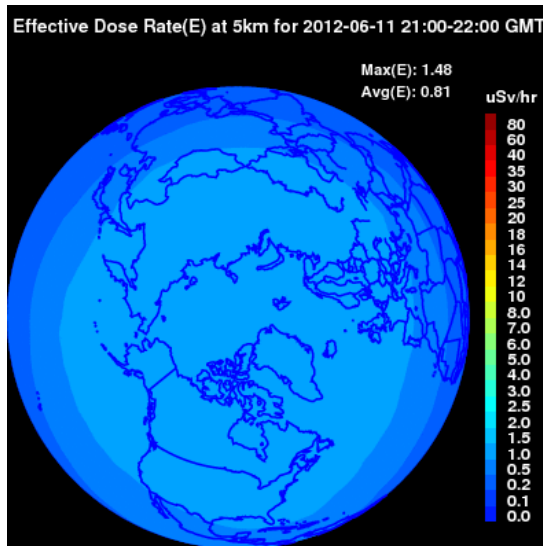
3.2b: Biological Effects of Cosmic Radiation: Commercial and Military Aviation Environments: Effect of Solar Particle Events on Aircrew Dose Rates

NAIRAS model - Halloween 2003 Geomagnetic Storm and Solar Particle Event Analysis
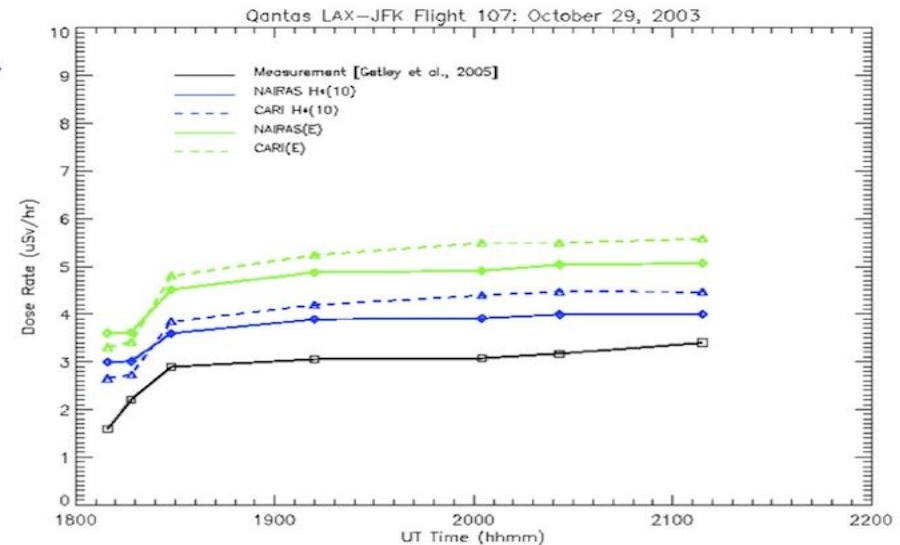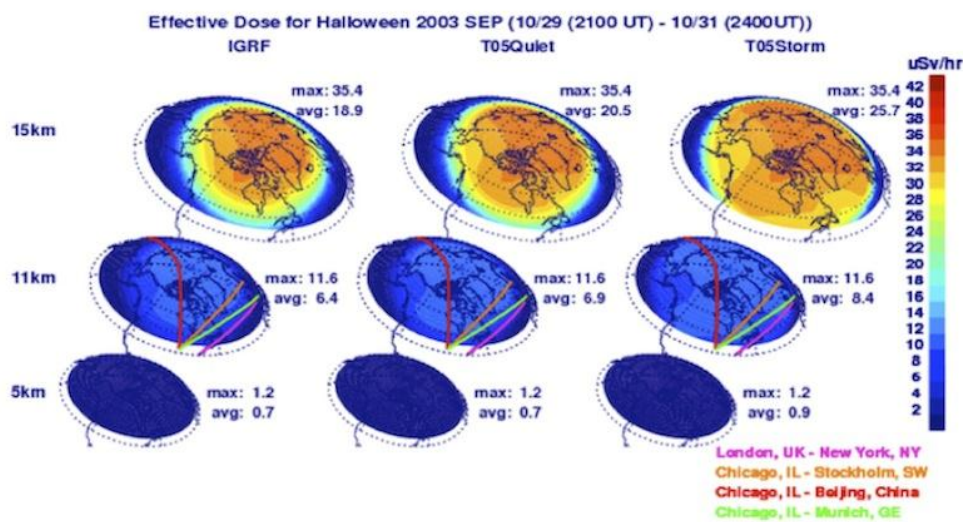
The figure at right shows the NAIRAS prediction of the radiation exposure quantity related to biological risk - Effective dose rate (uSv/hr). To put the exposure rates into perspective, one chest X-ray is about 100 uSv, and a CT scan is about 8,000 uSv. The exposure rate on ISS ≅ 18-20 μSv/hr.
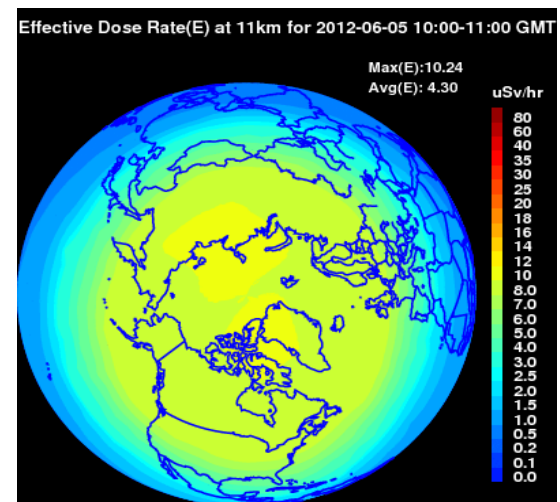
3.3a Biological Effects of Cosmic Radiation – Manned Space Flight Environments

CREW DOSE LIMITS

GUIDELINES

- **Code of Federal Regulations**
- **Crew & Area Dosimetry**
- **ALARA – "As Low As Reasonably Achievable"**
- **NASA Flight Rules, e.g., No EVAs in South Atlantic Anomaly**
- **Crew annual and career dose limits**

Dose limits (cGy-Eq.) for short-term or career non-cancer effects*

Organ	30-Day Limit	1-Year Limit	Career
Eye (Lens)	100	200	400
Skin	150	300	600
BFO	25	50	---
Heart	25	50	100
CNS	50	100	150

BFO – BLOOD-FORMING ORGAN
CNS – CENTRAL NERVOUS SYSTEM
cGy-Eq. (centi Gray-Equivalent $\cong$ cSv (centi Sievert)

***NASA STD 3000 (1994) & NCRP Report No. 132 (2000)**

-Based on a limit of 3% radiation exposure induced (premature) death (REID) with 95 % confidence level (Code of Federal Regulations)

-Also, the new Crew Exploration Vehicle (CEV) design objective is 150 mSv per year, down from historical 500 mSv per year as driven by uncertainty in the dose-REID relationship in the primary CR dominated space radiation environment

3.3b Biological Effects of Cosmic Radiation – Manned Space Flight Environments

Spaceflight Radiation Examples - Human Spaceflight Mission Type Radiation Dose:

Assuming 20 to 50 g/cm^2 Al shielding and not including secondary particle shower effects internal to the human body which can increase effective dose by about 50%

Space Shuttle Mission 41-C	**5.59 mSv**
(8-day mission orbiting the Earth at 460 km)	
Apollo 14	**11.4 mSv**
(9-day mission to the Moon)	
Skylab 4	**178 mSv**
(87-day mission orbiting the Earth at 473 km)	
International Space Station (ISS) Mission	**160 mSv**
(up to 6 months orbiting Earth at 353 km)	
Estimated Mars mission (3 years)	**1200 mSv**

Slow accumulation of whole body dose from GCR (expressed in Effective equivalent Sv) and including secondary particle showers in the human body) presently limits the duration of manned space operations outside earth's magnetosphere to times on the order of 180 days (assuming 20 to 30 g/cm^2 shielding mass). The overall programmatic cost of the available active or passive shielding needed to extend that limit is likely prohibitive at this time (Francis A. Cucinottaa, Myung-HeeY. Kim, Lei Ren; "Evaluating shielding effectiveness for reducing space radiation cancer risks," Radiation Measurements 41 (2006) 1173 – 1185)

Spacecraft shielding mass estimates for career dose limits of: 1) 150mSv (x - new) and 2) 1000 mSv (Δ - old) and mission durations of 1 to 4 years (median atmospheric shielding mass)
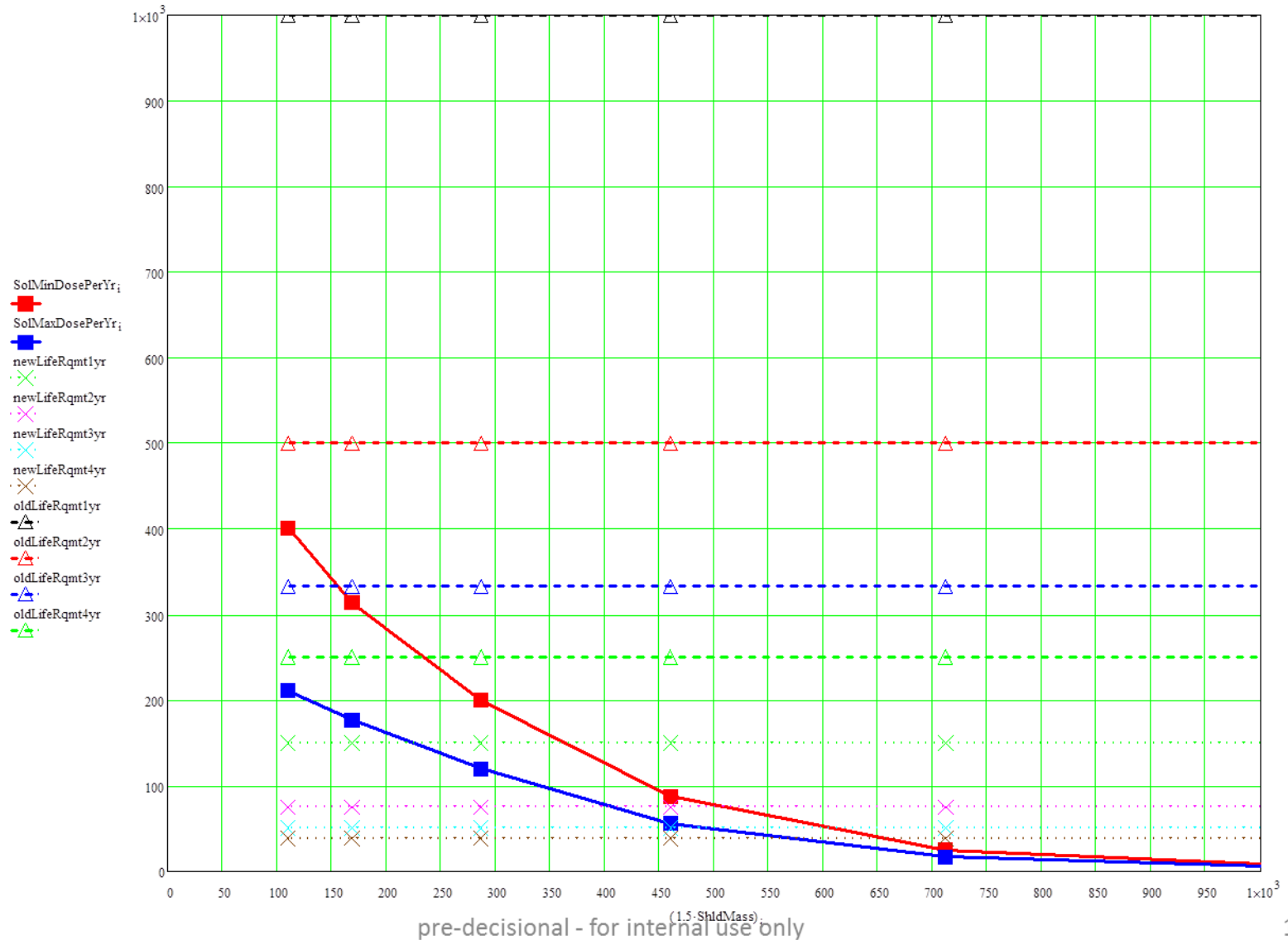
NASA HZETRN 2010 estimates of crew dose vs. shielding mass for a 3 year interplanetary mission assuming solar Maximum and solar minimum GCR environments and no SEP event contributions and both the 10 and 100 cSv career dose limits.
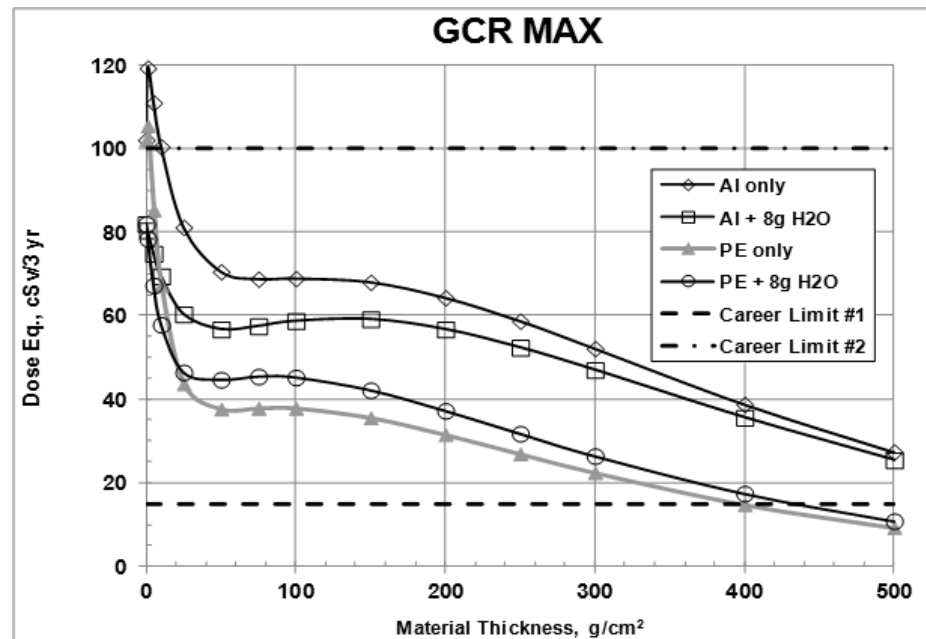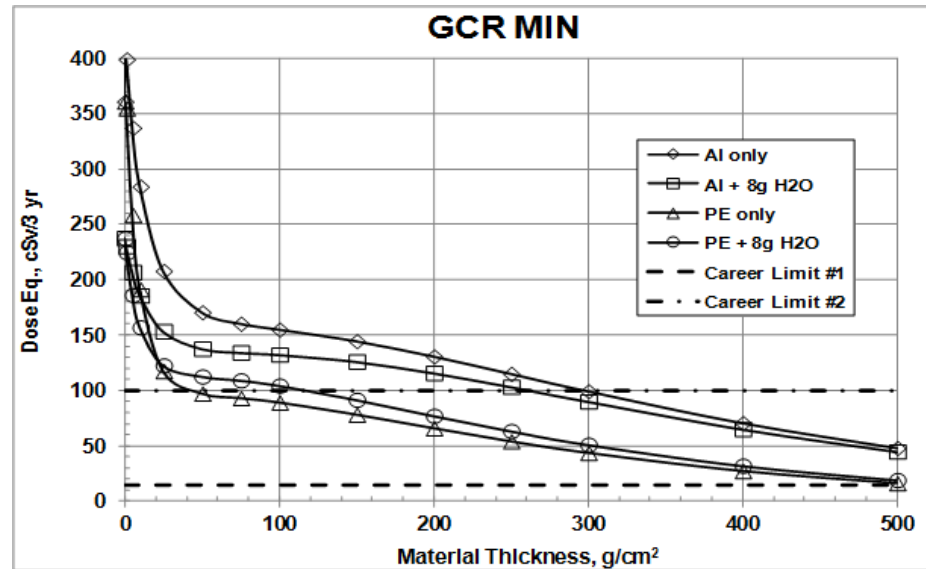
Assumed Hybrid DSH Dimensions

- Pressurized Core Volume (excludes any inflatable envelope outside)
  - Cylinder
    - 4.5 meters (450 cm) diameter
    - 6 meters (600 cm) long
    - Volume = 95.43 cubic meters
    - Lateral surface area = 8.48 x 10^5 square centimeters
    - Total end cap surface area = 3.18 x 10^5 square centimeters
- Crew quarters located on one end of the pressurized core volume
  - Cylinder
    - 4.5 (450 cm) meters diameter
    - 3 meters (300 cm) long
    - Volume 47.7 cubic meters
    - Lateral surface area 4.24 x 10^5 square centimeters
    - End cap (2 of) surface area = 3.18 x 10^5 square centimeters

Shielding mass total (kg) for a specific DSH hybrid habitat (minimum atmospheric shielding mass estimate)

Mission Duration (years)	150 mSv/career Hybrid Hab kg	150 mSv/career Crew Quarters kg	1000 mSv/career Hybrid Hab kg	1000 mSv/career Crew Quarters kg
1	2.916×10^5	1.856×10^5	3.499×10^4	2.227×10^4
2	4.082×10^5	2.598×10^5	5.832×10^4	3.711×10^4
3	4.782×10^5	3.043×10^5	1.166×10^5	7.422×10^4
4	5.248×10^5	3.340×10^5	1.749×10^5	1.115×10^5

Note – The basic Hybrid DSH spacecraft total wet mass (w/PMR) is estimated at 2.9×10^4 kg for the MSFC 60 day scenario and at 4.6×10^4 kg for the MSFC 500 day scenario. Spacecraft total wet mass is not a significant fraction of the shielding mass requirement for the 150 mSv career limit cases, but may contribute significantly to meeting the shielding mass requirement for the 1000 mSv career limit cases.

Shielding launch cost for a specific DSH hybrid habitat: @ $22,000 (see charts 45 and 46) per kg to GTO (minimum shielding mass estimate)

Mission Duration (years)	150 mSv/career Hybrid Hab $	150 mSv/career Crew Quarters $	1000 mSv/career Hybrid Hab $	1000 mSv/career Crew Quarters $
1	7.3×10^9	4.6×10^9	8.7×10^8	5.6×10^8
2	1.0×10^{10}	6.5×10^9	1.5×10^9	9.3×10^8
3	1.2×10^{10}	7.6×10^9	2.9×10^9	1.9×10^9
4	1.3×10^{10}	8.4×10^9	4.4×10^9	2.8×10^9

Combinations with launch costs less than ~ 2 billion dollars are highlighted in red

Shielding launch cost for a specific DSH hybrid habitat @ $5,000 per kg to LEO (minimum atmospheric shielding mass estimate)

Mission Duration (years)	150 mSv/career Hybrid Hab $	150 mSv/career Crew Quarters $	1000 mSv/career Hybrid Hab $	1000 mSv/career Crew Quarters $
1	1.458×10^9	9.278×10^8	1.749×10^8	1.113×10^8
2	2.041×10^9	1.299×10^9	2.916×10^8	1.856×10^8
3	2.391×10^9	1.522×10^9	5.832×10^8	3.711×10^8
4	2.624×10^9	1.670×10^8	8.747×10^8	5.567×10^8

Combinations with launch costs less than 2 billion dollars are highlighted in red. Note the cost benefit of building the spacecraft in LEO for departure from LEO (or launching to LEO and transporting to an earth-moon LaGrange point using relatively low cost ($1 to $3 billion) reusable solar electric tugs) !

6.0 Summary & Conclusions

- The effects of energetic cosmic ray, solar particle event, and trapped radiation charged particles on contemporary electronic systems as well as human health and safety depends on:
  - The production of ionization/excitation tracks in target materials
  - Collisions with target material nuclei to initiate secondary particle showers
- CR secondary particle shower species, especially neutrons, dominate effects on electronic systems and human health at high shielding mass
  - Earth surface operating environments
  - High altitude aircraft operating environments
  - Heavily shielded manned spacecraft
  - In massive targets, like the human body, secondary particle showers can contribute on the order of 50% of the total body dose expressed in Sv
- SEE effects on electronic systems can be managed by: 1) selection of resistant parts, 2) EDAC and FDIR functions, and 3) robust/highly redundant system architectures
- Shielding mass can mitigate electronic system TID and SEE effects from SPE and trapped radiation but is largely ineffective against GCR
- Slow accumulation of whole body dose (expressed in Sv) from GCR presently limits the duration of manned space operations outside earth's magnetosphere to times on the order of 180 days. The overall programmatic cost of the available active or passive shielding needed to extend that limit is prohibitive at this time

5.0 Supporting Data: Modeling and Calculation Methods

Energetic Particle Interactions with Materials

Direct ionization & excitation of target substance

- **High speed charged particles decelerate by loosing energy to target substance electrons during columbic collisions leaving an ionization/excitation damage track**
  - ◆ Nuclear collisions make little contribution to deceleration except at the lowest kinetic energies near end of track.
  - ◆ http://pdg.lbl.gov/2010/reviews/rpp2010-rev-passage-particles-matter.pdf
- **dE/dx is the rate of energy transfer: keV/micron or MeV-cm^2/mg in a particular target substance**
  - ◆ Linear and nearly constant over most of the particle range - hence the term linear energy transfer (LET)
  - ◆ Nonlinear near end of track – most of the energy is deposited near the end of track in the "Brag Peak"; basis of accelerator hadron therapy for certain cancers
- **Quantified by the relativistic Bethe-Bloch equation**

$$-\frac{dE}{dx} = \frac{4\pi}{m_e c^2} \cdot \frac{n z^2}{\beta^2} \cdot \left(\frac{e^2}{4\pi\varepsilon_0}\right)^2 \cdot \left[\ln\left(\frac{2m_e c^2 \beta^2}{I \cdot (1-\beta^2)}\right) - \beta^2\right]$$

Projectile (cosmic ray particle) dependencies

$\beta = v/c$; v = velocity of the particle; E = energy of the particle; x = distance travelled by the particle in the target; c = speed of light; z = particle charge; ε_0 = vacuum permittivity

Target substance dependencies

I = mean excitation potential of the target = 10eV(Z), n = electron density of the target = $(N_A Z \rho)/A M_\mu$; ρ = density of the target; Z = target atomic number; A = target atomic mass number; N_A = Avogadro number; and M_u = Molar mass constant = 1 in Si units; e = charge of the electron; m_e = rest mass of the electron
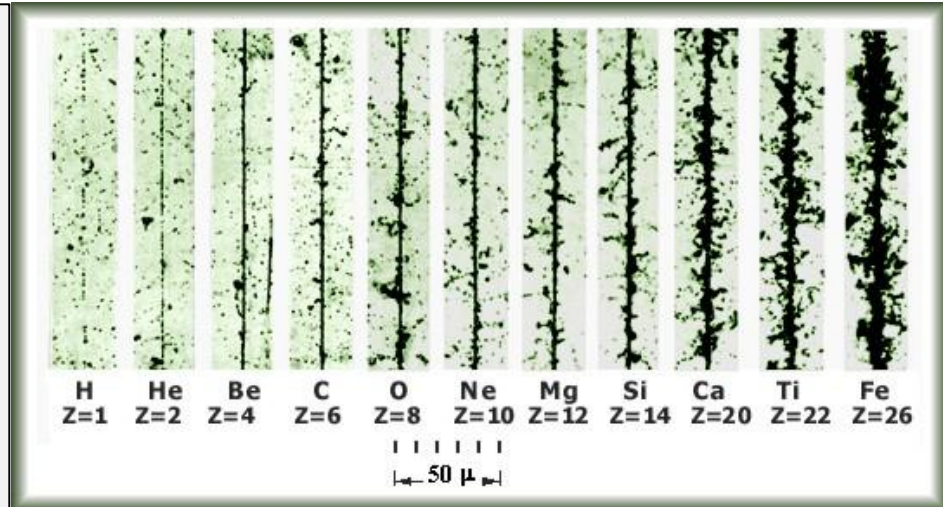
Photographic/nuclear emulsion tracks - Image Credit - PROF. P. FOWLER, UNIVERSITY OF BRISTOL
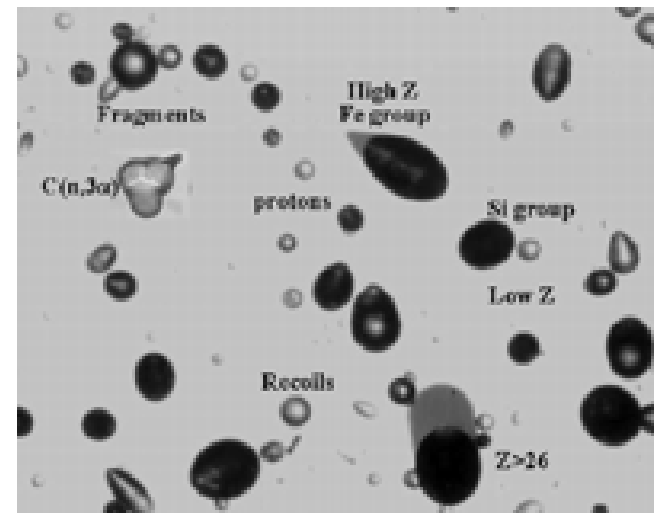
CR-39 (polycarbonate thin plastic sheet) solid state nuclear track detector SSNTD – ISS Tracks are revealed by etching the plastic post flight

Nuclear Reactions and Secondary Particle Showers

- **Inelastic collisions attenuate the primary flux exponentially and generate secondary particle showers via nuclear reactions**
 - **$N(l) = N(0) \exp(-l/\lambda)$**
    - λ = inelastic collision length (grams/cm^2)
    - l = thickness in g/cm^2
  - **http://pdg.lbl.gov/2010/reviews/rpp2010-rev-atomic-nuclear-prop.pdf**
    - λ ranges from **42 g/cm^2 to 118 g/cm^2 for protons in various materials**
    - At fixed target mass, number of collisions decreases with increasing atomic weight (i.e. fewer target nuclei per gram)
    - λ Scales as **(projectile atomic number)$^{0.77}$**
    - λ increases with target atomic number
- **$\langle n_{event} \rangle$ = average number of secondary particles per collision event**
- **$\langle n_{collision} \rangle$ is proportional to A(projectile) x A(target) x (average nuclear thickness function)**
- **$\langle n_{shower} \rangle$ is proportional to primary projectile energy**
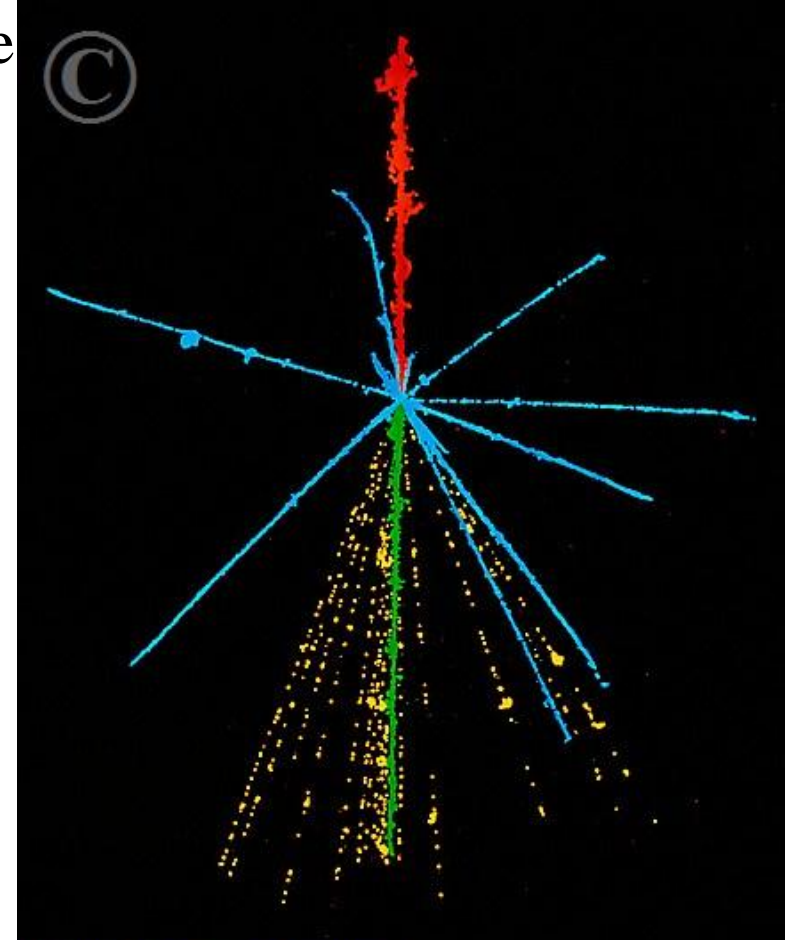
a134005 [RM] © www.visualphotos.com

False- color emulsion photo of a cosmic ray sulfur nucleus (red) colliding with a nucleus in the emulsion. The collision produces a spray of other particles: a fluorine nucleus (green), other nuclear fragments (blue) & 16 pions (yellow). The length of the sulfur track is 0. 11 mm. The curlicues which adorn the track of the sulfur nucleus are electrons which it has knocked out of atoms in passing. The photograph was taken in 1950 by Cecil Powell, the English physicist who pioneered the use of photographic emulsions to record the tracks of electrically charged particles.

Solid State Devices as Charged Particle Detectors

- **1) Solid state electronic devices as charged particle detectors: Single Event Effects (SEE)**
  - Solid state ionizing radiation detectors and most modern microelectronic devices share a common basic physical feature – the reverse biased P-N junction and corresponding depletion region.
  - Energetic charged particles traversing the device depletion region cause ionization, i.e. a large number of mobile charge carriers, along the particle track
  - The applied reverse bias voltage rapidly collects the mobile charge carriers so that:
    - A current pulse appears in the external circuit
    - The voltage across the depletion region collapses briefly and that voltage appears as a voltage pulse elsewhere in the external circuit leading to data corruption or even hardware failure
- **2) Solid state electronic devices as charged particle detectors: Total Ionizing Dose (TID) Effects**
  - Driven by accumulation of trapped charge in SiOx isolation layers in the device
  - Both Si based bipolar and Si based MOS Technologies are affected
  - Accumulation of trapped charges in SiOx layers leads to changes in device characteristics and eventually device failure
  - TID to failure varies widely with device type, elemental composition, and device architecture – SiOx layer location and thickness is important for Si devices
  - Failure dose ranges from 10^3 rad (Si) to more than 10^7 rad (Si) depending on the degree of TID hardening by design for each device type and elemental composition

CR effects on human health and safety

- **Exposing cells to ionizing radiation leads to lethality, mutation induction, and carcinogenesis**
- **Primary and secondary cosmic ray particles transfer energy, proportional to charged particle LET = dE/dx, to atoms and molecules in the cellular structure along the particle ionization track so as to:**
  – Produce free radicals
  – Break chemical bonds
  – Produce new chemical bonds and cross-linkage between macromolecules
  – Damage molecules and molecular assemblies that regulate vital cell processes (e.g. DNA, RNA, proteins, and membrane lipid structures)
- **Ionizing radiation induces both direct biomolecule damage and indirect biomolecule damage through the radiolysis of water.**
  – At low doses (i.e. damage rates), such as what we receive every day from background radiation, the cells repair the damaged molecules rapidly enough to survive
  – At higher doses (up to 1000 mSv), the cells might not be able to repair the damage rapidly enough , and the cells may either be changed permanently or die.
- **Cells changed permanently may go on to produce abnormal cells when they divide. In the right circumstance, these cells may become cancerous. This is the origin of our increased risk in cancer, as a result of radiation exposure.**
  – Bystander cells can also be affected via intracellular signal transduction pathways

DNA

Direct effect

Indirect effect

$H_2O^+ + e^- \curlyvee H_2O$

$\downarrow$

$OH^- + H_3O^+ + e^-_{aq}$

DNA repair

Cell cycle checkpoint control

Cell survives and proliferates

Secreted soluble factors

Cell-Cell gap junction communication

A   B

http://www.pnas.org/content/102/40/14127/F1.large.jpg

35
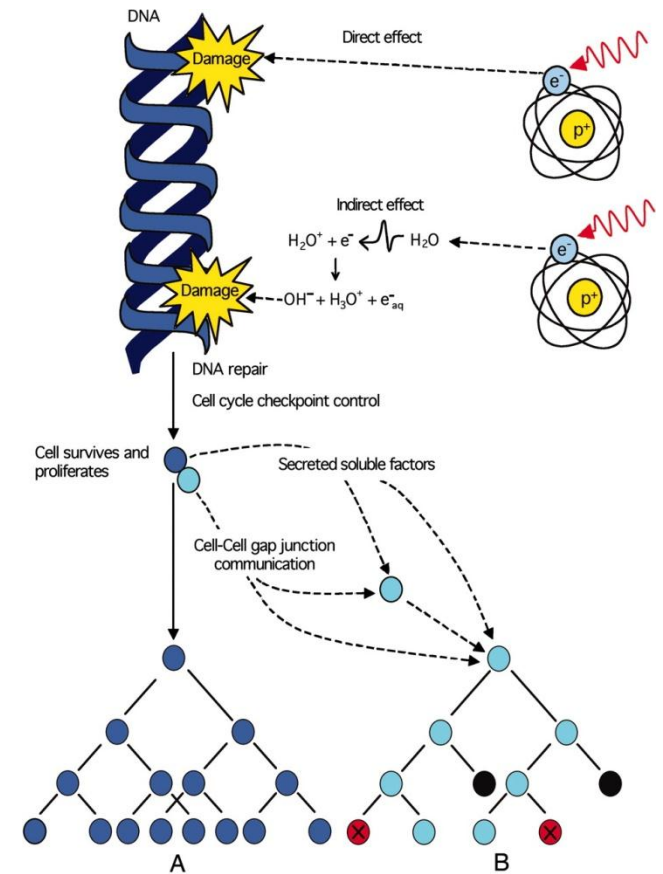
Natural Environment Definitions: CREME 96, Peterson Figure of Merit, and FLUKA Natural Environment Parameters

- CREME 96 and FOM input natural environments for calculations (16)
  - GEO/Interplanetary Fluxes, Solar Minimum, Z=1-92
  - ISS: 362km/51.6°, Solar Minimum,
  - GCR environment based on "A Model of Galactic Cosmic Ray Fluxes", by R.A. Nymmik, M.I. Panasyuk, T.I Pervaja, and A.A. Suslov, Nuclear Tracks and Radiation Measurements, 20, 427-429 (1992)
- FLUKA input natural environments for calculations
  - Uses a subset of the CREME-96 Environments as shown below
    - H, He, C, O, Mg, Si, Fe
    - Accounts for 98 % + of total GCR flux
    - Increases computational speed and efficiency with negligible impact on accuracy

FLUKA Methods Overview

- FLUKA Monte Carlo nuclear reaction and transport code (1)
  - Theory driven and benchmarked with data - Based on original and verified microscopic interactions models
    - FLUKA is not a tool kit, rather a transport code with fully integrated physics models
    - First principle model – no adjustable parameters – does not rely on extrapolated empirical look-up tables
      - Nucleus-nucleus interactions from 100 MeV/n to 10000 TeV/n
      - Hadron-hadron and hadron-nucleus interactions 0–10000 TeV
      - Exact dE/dx ionization (LET) calculation with delta ray production and statistical fluctuations
      - No limitation on projectile/target composition or combination
- Simple 3D spacecraft model
  - Concentric spherical shells – simple shielding mass distribution function for each shell
    - 10 μ thick Si "detector" shells at various shielding mass depths – optional 1 μ metallization layers on outward facing Si shell surface (a generic microelectronic device structure)
    - Report TID and nuclear reaction rates for each Si or metallization shell
    - Report LET spectra entering outward facing surface of Si detector shell
- SEE rate calculations
  - Calculate SEE rates with:
    - Differential LET spectrum entering each Si detector shell at each shielding depth in the concentric sphere structure (Includes all secondary particle production in "spacecraft shielding mass and metallization layers)
    - Directional cross section function, $\sigma(LET,\Theta,\Phi)$, from device heavy ion test data
  - Same $\sigma(LET,\Theta,\Phi)$ in FLUKA, CREME-96, and Petersen Figure of Merit (FOM) calculations

FLUKA 2008.3b Calculation Details – Detector Shell Configuration

- Spacecraft shielding simulated using FLUKA 3D concentric spherical shells

- 10 micron Si detector shells are inserted at different shielding depths with optional 11 micron heavy element shells (over-layers) on the silicon shells

- Each concentric shell is a FLUKA "region" with specific boundary surfaces.

- The volume of the sphere at radii smaller than 5000 cm is treated as a perfect particle absorber in all FLUKA calculations reported here.

- FLUKA reports the number of particles of LET X entering the 10μ Si detector shells per primary particle, as well as the number of nuclear reactions and total energy deposition (TID), also per primary particle, internal to each of the concentric spherical shell shielding shells, 10μ Si shells, or 1μ metal shells on the Si shells.

FLUKA 2008.3b Calculation Details – Detector Shell Shielding Mass

- FLUKA launches randomly directed energetic particles into the 3D concentric spherical model spacecraft structure, thereby sampling the full shielding mass distribution function of the model
  - Simulates an isotropic particle flux on a concentric spherical shell structure.
- The shielding mass distribution function metrics (Table 1 below) corresponding to each of the 10μ Si detector shells (or 1μ over layer shells) are used for data reporting and comparison.
- Example – shielding mass distribution function metrics values in g/cm^2 Al for each Si shell in the concentric spherical spacecraft model. Metrics for another shielding material, X, can be obtained by multiplying the density ratio, ρ_x/ρ_{Al}

FLUKA Target	SiDet1	SiDet2	SiDet3	SiDet4	SiDet5	SiDet6	SiDet7	SiDet8
Spherical shell minimum shielding mass thickness (along the radius) in g/cm^2	0.1	0.5	1.0	5.0	10.0	20.0	50.0	100
Spherical shell median shielding thickness, with geometric cosine correction only, in g/cm^2	0.14	0.70	1.40	6.90	13.7	27.3	68.1	137.2
Spherical shell median shielding thickness, with cosine and solid angle corrections, in g/cm^2	0.15	0.81	1.6	7.9	15.6	31.1	77.5	156.2

Spacecraft shielding mass and secondary particle shower effects are calculated using the **FLUKA** (**FLU**ktuierende **Ka**skade) (ref. 1) Monte Carlo nuclear reaction and transport code applied to a hollow concentric spherical shell spacecraft model and the natural LEO and interplanetary primary particle environments on the previous slide

The generic spacecraft structure model consists of a hollow spherical shell structure (shown in cross section to the right) with an inner radius of 5000 cm and an outer radius of 5037 cm.

Various thicknesses of Al shielding material overlay eight thin Si detector (scoring shells) labeled SiDet1 to SiDet 8, moving from the exterior of the sphere to the interior. See Table 1 for the median Al shielding mass overlying each Si detector shell.
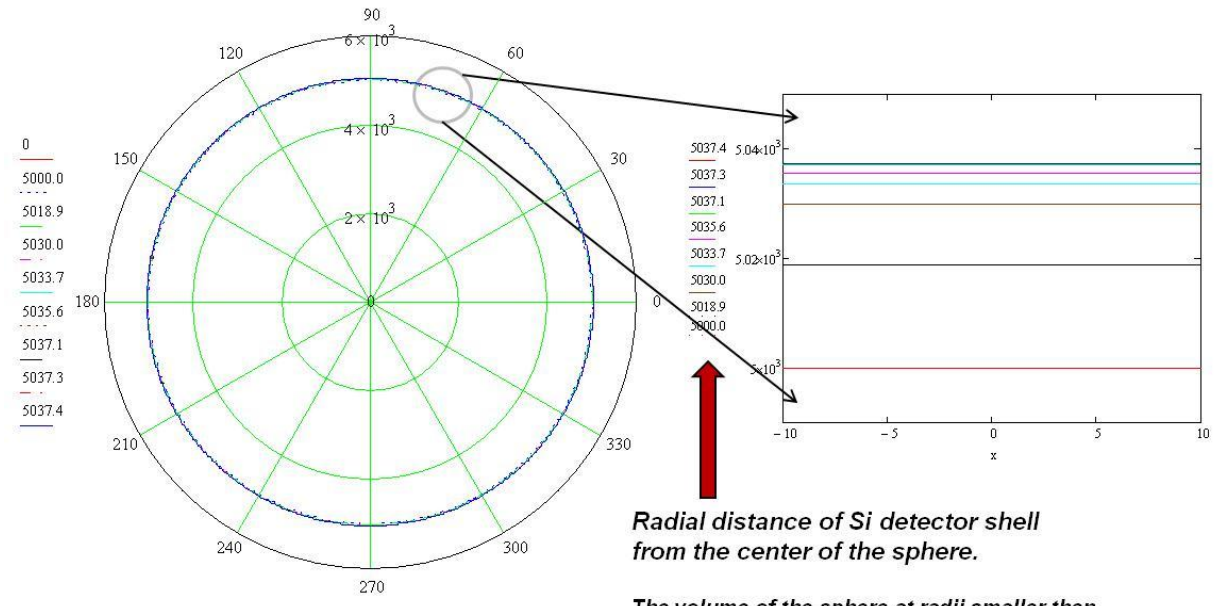

Radial distance of Si detector shell from the center of the sphere.

The volume of the sphere at radii smaller then 5000 cm is treated as a perfect particle absorber in all FLUKA runs

Table 1

Detector Si Shell	SiDet1	SiDet2	SiDet3	SiDet4	SiDet5	SiDet6	SiDet7	SiDet8
Detector Shell Radius (cm)	5037.4	5037.3	5037.1	5035.6	5033.7	5030.0	5018.9	5000.0
Si Detector Median Al Shielding Mass in g/cm²	0.15	0.81	1.6	7.9	15.6	31.1	77.5	156.2

Steve Koontz, Brandon Reddell, Paul Boeder: "Calculating Spacecraft single Event Environments with FLUKA, Paper W-33, Proceedings of the 2011 NSREC Radiation Effects Data Workshop, IEEE, July 2011

FLUKA 2008.3b Calculation Details - Estimating the in-flight SEU rate from the FLUKA LET Spectrum and the Device Heavy Ion Test Data

- FLUKA simulations produce the differential form of the LET spectra entering each 10μ Si shell
  - Forward going particles only reported here – backward going particle fluxes are also calculated, but do not contribute significantly to the result
  - FLUKA "USRYIELD" utility used to recover LET spectra of particles crossing boundaries
  - Results reported on a per geometric region or region boundary and per primary particle basis
  - Scaling to on-orbit primary particle flux/fluence

- Use the integral form of the microelectronic device directional cross section $\sigma(LET,\Theta,\Phi)$ and the following $\sigma(LET,\Theta,\Phi)$ approximations as determined by the test/flight data sources
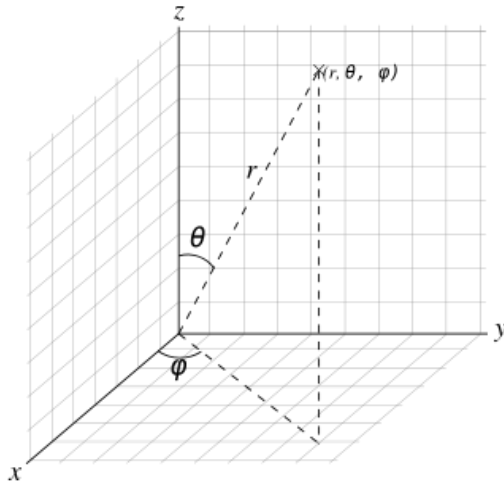
The x y plane is the plane of the microelectronic device die

- Θ and Φ define the entry angle of a particle in the microelectronic device coordinate system
- $\sigma(LET,\Theta,\Phi)$ represented as a simple geometric solid with a specific aspect ratio (width/thickness)
  - Isotropic Target, (17) $\sigma(L,\theta) = \sigma_N(L)$ for all θ sometimes observed especially for CMOS DRAM
  - Cosine Law Target, (17), $\sigma(L,\theta) = |\cos\theta| \sigma_N(L / |\cos\theta|)$ up to $\theta = 60$ degrees, commonly observed, (17)
  - Right Circular Cylinder (RCC) Target , (18-21). Note that we use the average (first moment) cord length for a given θ, not the full chord length distribution

- The on-orbit rate estimate is then given by: **Upset Rate = $\iiint$ f[LET] x $\sigma(LET,\Theta, \Phi)$ d(LET)d(Θ) d(Φ)**

FLUKA 2008.3b Calculation Details - Estimating the in-flight SEU rate from the FLUKA LET Spectrum and the Device Heavy Ion Test Data

- Estimating Total Ionizing Dose (TID) and nuclear reaction (star) rates per unit volume
  - FLUKA "SCORE" utility reports total ionizing dose and nuclear reactions ("stars") caused by all:
    - Protons
    - Neutrons
    - Pions
  - SCORE also reports expected in-flight total ionizing dose and "star" density using concentric spherical shell model dimensions and with scaling to on-orbit primary particle flux/fluence values
- How do we know all this works (method validation/success metric)?
  - Calculate least squares error metric – Σ(in-flight rate - estimated rate)^2 as a generic quality assessment of the various SEE rate estimate methods
  - If in flight rate predictions are within "a factor of a few" of the pre-flight predictions the method is usually considered more than adequate for practical work (17)
  - As a minimum, the on-orbit SEE rate calculation method should provide SEE rate estimates accurate to within a factor of 10 at one standard deviation when compared to available in-flight data (22-24)
- Run-to-run variability and error bars in Monte Carlo calculations
  - Monte Carlo models simulate real physical experiments or measurements including natural (random) quantum and statistical fluctuations, so the results of two statistically independent runs are not expected to be equal.
  - As is the case for radioisotope decay, and other Poisson processes, the uncertainty in a Monte Carlo particle or event count is equal to the square root of the number of particles or events in the result
  - In the following, plot symbols are always selected to be larger than or equal to the expected error of the numbers plotted unless two statistically independent FLUKA runs are plotted, in which case the error plot represents the spread in the data points directly
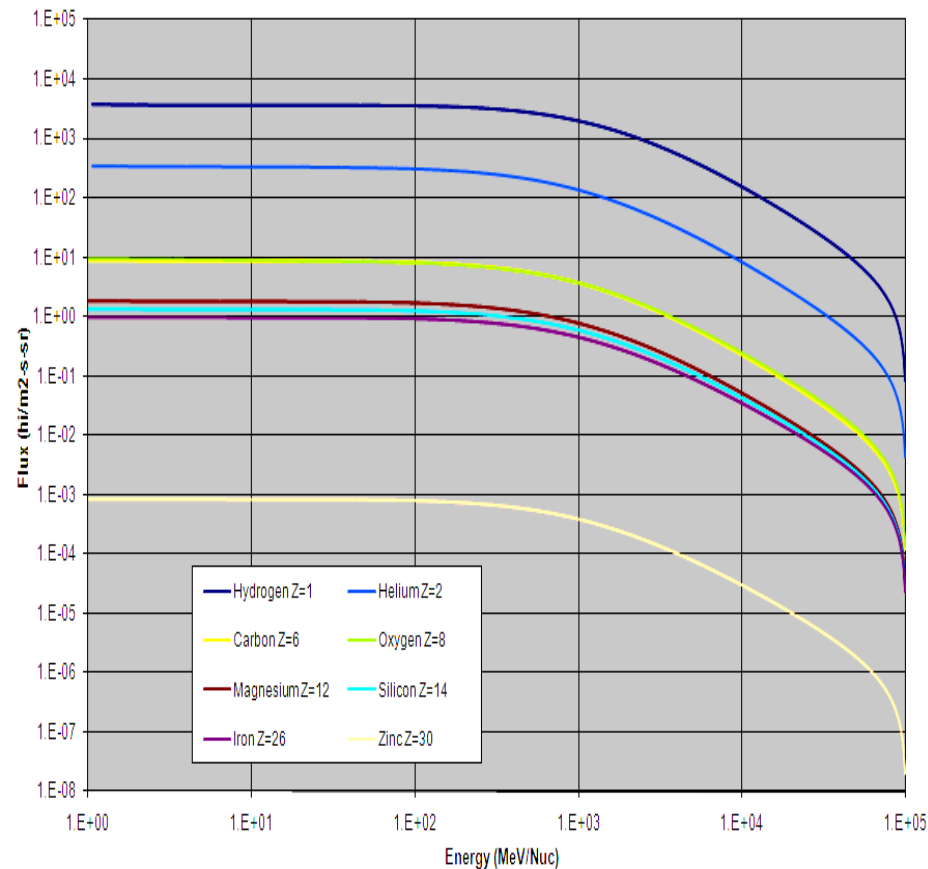
Device Parameters

Device	FLUKA RCC / ISO/Cosine law	CREME96 RPP x,y,z (um)	Onset (MeV-cm2/mg)	Width (MeV-cm2/mg)	Exponent	Limiting XS (um2)
IMS1601EP	Cosine Law	39.5, 39.5, 5.92	2.75	140	0.95	1560
ISS TMS44400 1Mx4 DRAM	RCC (T/W 1)	5.48, 5.48, 5.48	0.99	7.7	1.3	30
ISS KM44S32030T 128Mbit SDRAM High	RCC (T/W 0.1)	2.42, 2.42, 0.24	13	30	1	5.859
ISS KM44S32030T 128Mbit SDRAM Low	RCC (T/W 0.1)	1.25, 1.25, 0.125	14	30	1	1.563
ISS KM44S32030T 128Mbit SDRAM Koga	RCC (T/W 0.1)	0.43, 0.43, 0.043	1.95	30	1.9	0.186
V4 XQR4VFX60 – BRAM	RCC (T/W 2)	1.87, 1.87, 3.74	0.2	70	0.724	3.5
V4 XQR4VFX60 – Config. Memory	RCC (T/W 2)	5.1, 5.1, 10.2	0.5	400	0.985	26
V5 LX330T – Config. Memory	RCC (T/W 2)	3.36, 3.36, 6.72	0.5	30	1.5	11.3
Thuraya DSP Megagate ASIC	ISO	2.5, 2.5, 1.76	2.7	20.6	1.2	6.3
Cassini OKI Solid State Recorder	ISO	6.32, 6.32, 6.32	0.5	32	3	40
SOHO SMJ44100 4Mx1	RCC (T/W 0.25)	7.07, 7.07, 2	0.7	15	2.7	50
SOHO MHS CP65656EV 32kx8 SRAM	RCC (T/W 0.25)	7.75, 7.75, 2	1.9	17	1.2	60
ETS-V PD4464D-20 64k SRAM (	RCC (T/W 0.05)	19, 19, 10	0.5	15	2.9	375

Cosmic Ray Exposure Environments: Low-Earth Orbit and Interplanetary Space at 1 AU
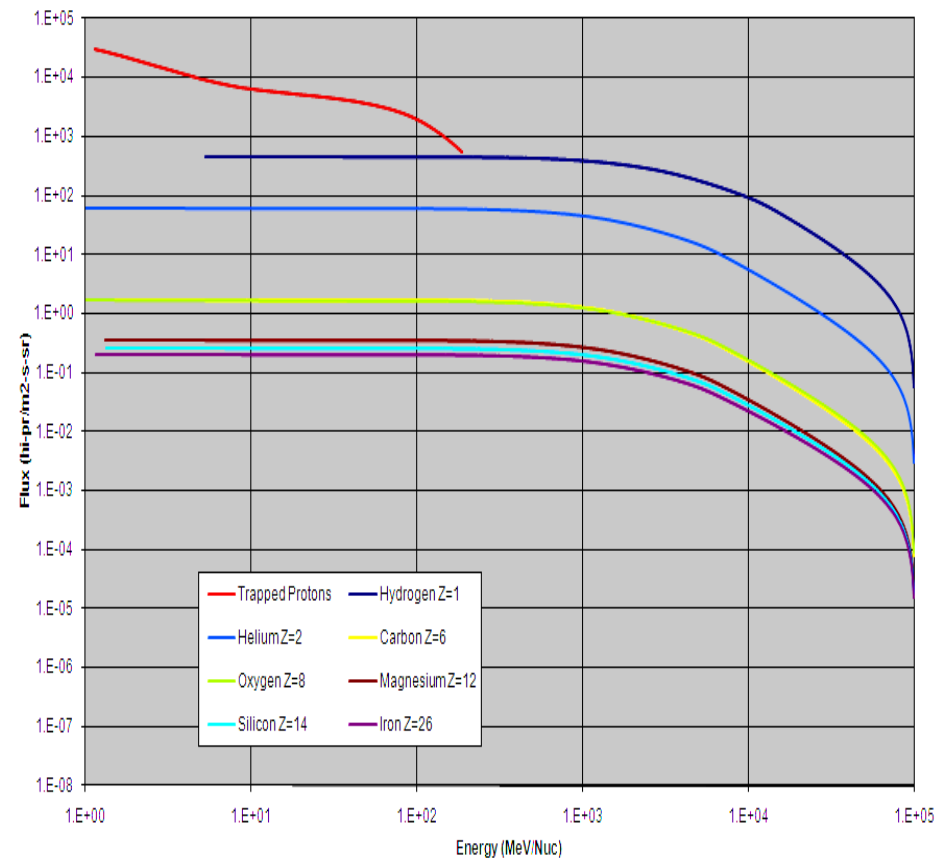## Eight most abundant GCR nuclei (98+% of total flux) and trapped protons

Steve Koontz, Brandon Reddell, Paul Boeder: "Calculating Spacecraft single Event Environments with FLUKA, Paper W-33, Proceedings of the 2011 NSREC Radiation Effects Data Workshop, IEEE, July 2011 as well as Refs 1 and 2

FLUKA Input: GCR Integral Flux in Free Space
(CREME96, Geosync, Solar Min=1977, Quit Conditions)

FLUKA Input: GCR Integral Flux at ISS Orbit
(CREME96, 362.5km, 51.6 Incl, Solar Min=1977, Quiet Conditions)

Interplanetary Environment at 1 AU: No geomagnetic shielding; direct solar particle event exposure; solar cycle modulation

Low-Earth orbit (ISS) environment: Latitude dependent geomagnetic shielding; Latitude dependent solar particle event exposure

In-flight vs. calculated spacecraft device SEU rates

Steve Koontz, Brandon Reddell, Paul Boeder: "Calculating Spacecraft single Event Environments with
FLUKA, Paper W-33, Proceedings of the 2011 NSREC Radiation Effects Data Workshop, IEEE, July 2011

For purposes of spacecraft design and verification, the agreement between the FLUKA based SEE
rate estimate sand the observed in-flight SEE upset rates are satisfactory, as shown below.

Spacecraft	Flight Env.	Ref.	Device	Median Shielding Mass g/cm^2	In-Flight SEU/bit day (X)	FLUKA (1) Predicted SEU/bit day (FLUKA)	CREME-96 (2) Predicted SEU/bit day (CREME)	FOM (3) Predicted SEU/bit day (FOM)
ISS	ISS	11-12	TMS44400	10	8.5×10^{-8}	8.8×10^{-8}	1.1×10^{-7}	2.5×10^{-7}
ISS	ISS	11-12	TMS44400	40	7.0×10^{-8}	7.2×10^{-8}	3.1×10^{-8}	6.8×10^{-8}
ISS	ISS	11-12	KM44S32030T-GL	40	3.3×10^{-10}	2.9×10^{-10}	1.9×10^{-10}	2.8×10^{-10}
ISS MISSE-7	ISS	13	V4 XQR4VFX60 - BRAM	0.8	4.2×10^{-8}	8.0×10^{-8}	8.6×10^{-8}	$6.8 X 10^{-9}$
ISS MISSE-7	ISS	13	V4 XQR4VFX60 – Config. Memory	0.8	3.8×10^{-9}	7.1×10^{-9}	9.1×10^{-9}	6.2×10^{-10}
ISS MISSE-7	ISS	13	V5 LX330T – Config. Memory	0.8	7.8×10^{-9}	6.5×10^{-9}	7×10^{-9}	1.9×10^{-8}
Space Shuttle	ISS	14	IMS1601EPI	34	3.1×10^{-7}	2.5×10^{-7}	2.7×10^{-7}	7.4×10^{-8}
Thuraya	GEO	15	ASIC 0.25 μ SRAM, IBM SA-12	0.7	5.3×10^{-8}	5.3×10^{-8}	7.9×10^{-8}	2.2×10^{-7}
Cassini	IP	16	OKI (4Mx1)	3.4	5.8×10^{-8}	2.5×10^{-8}	2.1×10^{-8}	1.9×10^{-7}
SOHO	IP	17	SMJ44100	1.0	5.9×10^{-7}	6.4×10^{-7}	1.2×10^{-6}	1.6×10^{-6}
ETS-V	GEO	18	PD4464D-20	5.8	1.7×10^{-6}	6×10^{-6}	9.3×10^{-6}	1.24×10^{-5}

A comparison of observed in-flight SPE SEU counts with estimates of SPE SEU counts calculated using the FLUKA radiation transport code and the concentric spherical shell spacecraft model

Steve Koontz, William Atwell, Brandon Reddell, Kristina Rojdev; NASA TP-2010-216133

For purposes of spacecraft design and verification, the agreement between the FLUKA based SPE rate estimate sand the observed in-flight SPE upset rates are satisfactory, as shown below.

Spacecraft/System and Device (ref)	Nov. 1997 SPE Upsets/bit	July 2000 SPE Upsets/bit	Nov. 2001 SPE Upsets/bit	Oct. 2003 SPE Upsets/bit
Cassini/Solid State Recorder DRAM (16) 1) Observed event upsets 2) Estimated event upsets 3) Estimated/Observed 4) Quiescent (no-event) daily upset rate	1) 4.4×10^{-7} 2) 1.4×10^{-7} 3) 0.32 4) 5.8×10^{-8}	NA	NA	NA
SOHO /Solid State Recorder DRAM (17) 1) Observed event upsets 2) Estimated event upsets 3) Estimated/Observed 4) Quiescent (n0 event)daily upset rate	1) 4.4×10^{-6} 2) $2.11 0^{-6}$ 3) 0.48 4) 5.9×10^{-7}	1) 4.7×10^{-5} 2) 2.1×10^{-5} 3) 0.4 4) 5.9×10^{-7}	NA	NA
Thuraya/ DSP DRAM (15) 1) Observed event upsets 2) Estimated event upsets 3) Estimated/Observed 4) Quiescent (no event) daily upset rate	NA	NA	1) 2.0×10^{-6} 2) 2.8×10^{-6} 3) 1.4 4) 5.3×10^{-8}	1) 1.5×10^{-6} 2) 3.8×10^{-6} 3) 2.5 4) 5.3×10^{-8}

Supporting Data: References & Device Parameters

Abstract

In this paper we review the discovery of cosmic ray effects on the performance and reliability of microelectronic systems as well as on human health and safety, as well as the development of the engineering and health science tools used to evaluate and mitigate cosmic ray effects in earth surface, atmospheric flight, and space flight environments.

Three twentieth century technological developments, 1) high altitude commercial and military aircraft; 2) manned and unmanned spacecraft; and 3) increasingly complex and sensitive solid state micro-electronics systems, have driven an ongoing evolution of basic cosmic ray science into a set of practical engineering tools (e.g. ground based test methods as well as high energy particle transport and reaction codes) needed to design, test, and verify the safety and reliability of modern complex electronic systems as well as effects on human health and safety.

The effects of primary cosmic ray particles, and secondary particle showers produced by nuclear reactions with spacecraft materials, can determine the design and verification processes (as well as the total dollar cost) for manned and unmanned spacecraft avionics systems. Similar considerations apply to commercial and military aircraft operating at high latitudes and altitudes near the atmospheric Pfotzer maximum. Even ground based computational and controls systems can be negatively affected by secondary particle showers at the Earth's surface, especially if the net target area of the sensitive electronic system components is large.

Accumulation of both primary cosmic ray and secondary cosmic ray induced particle shower radiation dose is an important health and safety consideration for commercial or military air crews operating at high altitude/latitude and is also one of the most important factors presently limiting manned space flight operations beyond low-Earth orbit (LEO).

6.1 References

1) G. Battistoni, S. Muraro, P.R. Sala, F. Cerutti, A. Ferrari, S. Roesler, A. Fasso`, J. Ranft, *"The FLUKA code: Description and benchmarking"* Proceedings of the Hadronic Shower Simulation Workshop 2006, Fermilab 6--8 September 2006, M. Albrow, R. Raja eds., and AIP Conference Proceeding 896, 31-49, (2007)  A. Fasso`, A. Ferrari, J. Ranft, and P.R. Sala, *"FLUKA: a multi-particle transport code"* CERN-2005-10 (2005), INFN/TC_05/11, SLAC-R-773

2) A. J. Tylka, J. H. Adams, Jr., P. R. Boberg, B. Brownstein, W. F. Dietrich, E. O. Flueckiger, E. L. Petersen, M. A. Shea, D. F. Smart, and E. C. Smith, "CREME96: A Revision of the Cosmic Ray Effects on Micro-Electronics Code", IEEE Trans. Nucl. Sci., vol. 44, no. 6, pp. 2150-2160, Dec. 1997.

3) Petersen, E. L., "The SEU Figure of Merit and Proton Upset Rate Calculations," IEEE Transactions on Nuclear Science, 45(6), December 1998, pp 2550-2562 (Section VII, p. 2557)

4) Holmes-Siedel, A., Adams, L.; <u>Handbook of Radiation Effects, Second Edition</u>, Oxford University Press, Oxford, New York, 2002

5) Clemens, M. A., Dodds, N. A., Weller, R. A., Mendenhall, M. H., Reed, R. A., Schrimpf, R. D., Koi, Y., Wright, D. H., Asai, M.; "The Effects of Nuclear Fragmentation Models on Single Event Effect Prediction," IEEE Transactions on Nuclear Science, 56(6), December 2009, pp 3158-2321-33164

6) Reed, R.A.; Weller, R.A.; Mendenhall, M.H.; Lauenstein, J.-M.; Warren, K.M.; Pellish, J.A.; Schrimpf, R.D.; Sierawski, B.D.; Massengill, L.W.; Dodd, P.E.; Shaneyfelt, M.R.; Felix, J.A.; Schwank, J.R.; Haddad, N.F.; Lawrence, R.K.; Bowman, J.H.; Conde, R., "Impact of Ion Energy and Species on Single Event Effects Analysis," IEEE Transactions on Nuclear Science, 55(4), December 2007, pp 2312-2321

7) Schrimpf, R.D.; Warren, K.M.; Ball, D.R.; Weller, R.A.; Reed, R.A.; Fleetwood, D.M.; Massengill, L.W.; Mendenhall, M.H.; Rashkeev, S.N.; Pantelides, S.T.; Alles, M.A., "Multi-Scale Simulation of Radiation Effects in Electronic Devices," IEEE Transactions on Nuclear Science, 55(4), August 2008, pp 1891-1902

8) Petersen, E. L., Pickel, J. C., Adams, J. H.; "Rate Predictions for Single Event Effects – A Critique," IEEE Transactions on Nuclear Science, 39(6), December 1992, pp 1577-1598

9) Petersen. E., L., "Predictions and Observations of SEU Rates in Space," IEEE Transactions on Nuclear Science, 44(6), December, 1997, pp 2174-2287

10) Petersen. E., L., "Parametric and Threshold Studies of Single Event Sensitivity," IEEE Transactions on Nuclear Science, 54(4), August 2007, pp 1392- 1405

11) Steve Koontz , Brandon Reddell, Paul Boeder: "Calculating Spacecraft single Event Environments with FLUKA, Paper W-33, Proceedings of the 2011 NSREC Radiation Effects Data Workshop, IEEE, July 2011

12) Falguere, D., Duzellier, S., Ecoffet, R., Tsourilo, I; "EQEX I-IV: SEE In-Flight Measurement on the MIR Orbital Station," IEEE Radiation Effects Data Workshop Proceedings, pp89-95, 2000.

13) Our thanks to Dave Bullington and Gayle Echo Thayer of Sandia National Labs for providing MISSE-7 FPGA SEU flight and ground test data

14) O'Neill, P., Badhwar, G.; "Single Event Upsets for Space Shuttle Flights of New General Purpose Computer Memory Devices," IEEE Transactions on Nuclear Science, 41(5), October 1994, pp 1755-1764

15) Hansen, D.L.; Jobe, K.; Whittington, J.; Shoga, M.; Sunderland, D.A, "Correlation of Prediction to On-Orbit SEU Performance for a Commercial 0.25-μm CMOS SRAM," IEEE Transactions on Nuclear Science, 54(6), December 2007, pp 2525-2533

16) Swift, G.M.; Guertin, S.M., "In-flight observations of multiple-bit upset in DRAMs," IEEE Transactions on Nuclear Science 47 (6) December 2000, pp 2386-2391

17) Harboe-Sorensen, R.; Daly, E.; Teston, F.; Schweitzer, H.; Nartallo, R.; Perol, P.; Vandenbussche, F.; Dzitko, H.; Cretolle, J., "Observation and analysis of single event effects on-board the SOHO satellite," IEEE Transactions on Nuclear Science, 49(3), June 2002, pp 1345- 1350

18) Goka, T.; Matsumoto, H.; Nemoto, N, "SEE flight data from Japanese satellites," IEEE Transactions on Nuclear Science 45(6) December 1998 , pp 2771-2778

19) Buttkewitz A., Duhm H. H., Goldenbaum F., Machner H., W. Strauss W.; "Fission Studies with 140 MeV Alpha Particles" http://arxiv.org/abs/0907.4042v1, arX1v:0907, 4042v1

20) James Rayford Nix, Elena Sassia,; "Estimates of the variation of nuclear fissilities throughout the periodic table," Nuclear Physics Volume 81, Issue 2, June 1966, Pages 61-70

21) R. Capote Noy; <u>Parameters for Calculation of Nuclear Reactions of Relevance to Non-Energy Nuclear Applications</u>, Summary Report of the First Research Coordination Meeting, IAEA Headquarters, Vienna, Austria, 23 – 25 June 2004, INDC(NDS)-462 Distr: G+NM

22) R. J. Peterson; "Nuclear Fission Induced by Pi Mesons," Journal of Nuclear and Radiochemical Sciences, Vol. 11, No.1, pp. R1-R19, 2010

GCR Exposure Environments – Earth's Atmosphere

- **Earth surface/atmospheric environments**
  - 1000 grams/cm^2 air shielding mass at sea level
  - latitude dependent geomagnetic shielding
  - GCR secondary particle shower products dominate

- **Commercial and military aviation environments**
  - Altitude dependent air shielding mass
  - latitude dependent geomagnetic shielding
  - Solar cycle modulation of GCR environment
  - Latitude dependent solar particle event exposure
  - Pfotzer secondary shower particle maximum at about 20 km altitude (mid latitudes)
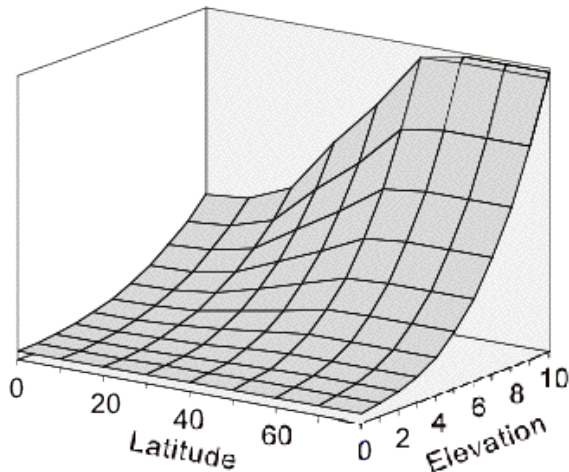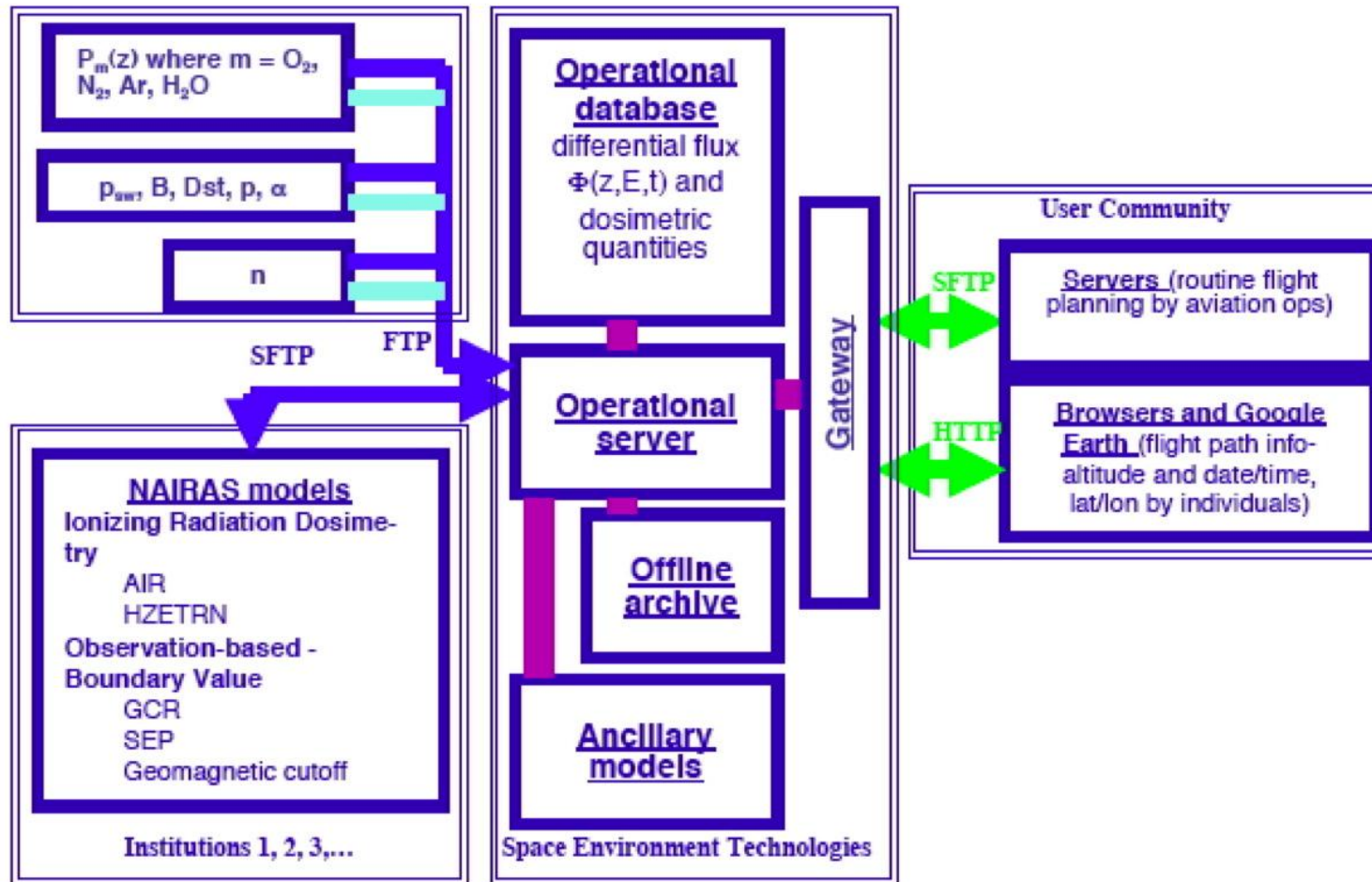

Relative variation of cosmic ray flux at the earth's surface as a function of altitude and latitude (Cosmogenic Nuclide Laboratory - University of Glasgow - http://web2.ges.gla.ac.uk/~dfabel/CN_explain.html)
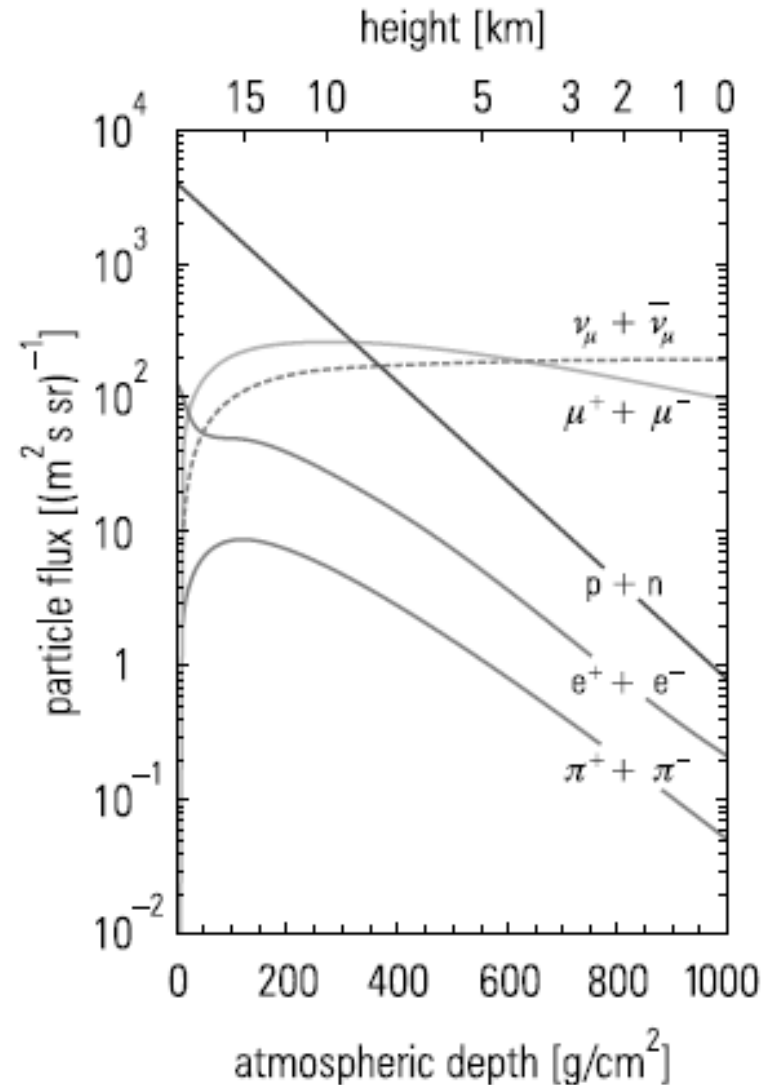
GCR secondary shower particle fluxes in Earth's atmosphere (http://pdg.lbl.gov/2011/reviews/rpp2011-rev-cosmic-rays.pdf)

NAIRAS* Operational Distributed Network System Architecture

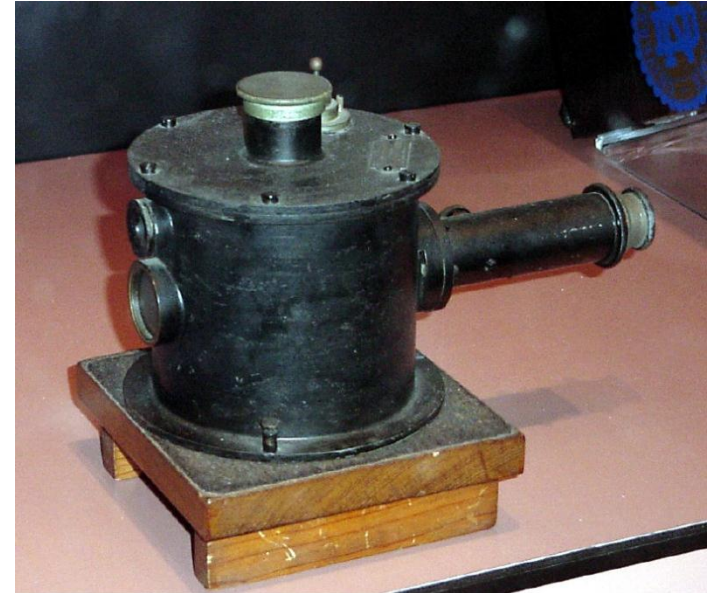http://sol.spacenvironment.net/~nairas/index.html

*NAIRAS - Nowcast of Atmospheric Ionizing Radiation for Aviation Safety

Discovery of GCR – observations from developing electrical technology (1785 to 1926)

- 1785 - Coulomb: reports spontaneous discharge

- 1835 - Faraday: confirms spontaneous discharge

- 1879 - Crooks: reduced discharge rate at reduced pressure

- 1896 - Bequerel/Curie: radioactivity discovered

- 1910 - Wolf climbs Eiffel tower with electroscope

- 1910 - Pacini: Discharge rate lower under water

- 1912 - Hess: After an initial drop, discharge rate increases steadily with altitude during balloon flights

- 1920s – Compton and Millikan: particles or photons?

- By 1926 a consensus was reached on what cosmic rays are (mostly energetic charged particles with some small number of energetic photons), and it all began with observations that capacitors can discharge in an unexpected way.

Victor Hess's Balloon Borne Electroscope
http://airandspace.si.edu/collections/artifact.cfm?id=A19910023000